DISCLAIMER NOTICE

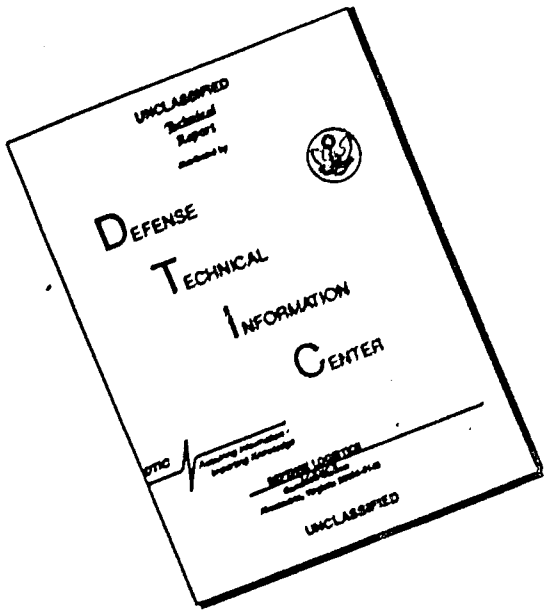

THIS DOCUMENT IS BEST QUALITY AVAILABLE. THE COPY FURNISHED TO DTIC CONTAINED A SIGNIFICANT NUMBER OF PAGES WHICH DO NOT REPRODUCE LEGIBLY.

DREXEL INSTITUTE OF TECHNOLOGY

PHILADELPHIA 4, PENNSYLVANIA

DIT Report No. 125-5

ATTENUATION OF THE STRONG PLANE SHOCK PRODUCED IN A SOLID BY HYPERVELOCITY IMPACT

by

PEI CHI CHOU

HARBANS S. SIDHU

LAWRENCE J. ZAJAC

Prepared for

Ballistic Research Laboratories
Aberdeen Proving Ground

under

Contract No. DA-36-034-ORD-3672 RD

February, 1964

DIT Report No. 125-5

ATTENUATION OF THE STRONG PLANE SHOCK PRODUCED IN A SOLID BY HYPERVELOCITY IMPACT

by

PEI CHI CHOU

HARBANS S. SIDHU

LAWRENCE J. ZAJAC

Prepared for

Ballistic Research Laboratories
Aberdeen Proving Ground

under

Contract No. DA-36-034-ORD-3672 RD

February, 1964

A B S T R A C T

The attenuation of strong plane shocks in solids produced by hypervelocity impact is studied, and two parametric equations are developed which describe the path of the shock front in the x,t-plane. These parametric equations were derived by considering the entropy change across the decaying shock and assuming that the characteristic lines behind the shock are straight lines. The equation of state is approximated by simple Hugoniot and isentrope equations. The same problem is also solved graphically by a stepwise characteristic method. A comparison of the graphical and analytical results shows that the simplifying assumptions made for the analytical solution are valid for both weak and strong shocks.

TABLE OF CONTENTS

LIST OF FIGURES

LIST OF TABLES

I. Introduction

In the theoretical study of hypervelocity impact, the hydrodynamic theory is generally recognized to be applicable in the high pressure region. Based upon this hydrodynamic theory, Walsh and Tillotson[1] and Bjork[2] have obtained numerical solutions by using finite-difference methods. Their results give a most detailed history of the properties and motions of material particles. However, the finite-difference methods have certain inherent deficiencies. Namely, they are not convenient for engineering application because each impact problem must be calculated separately on a computer with a large capacity. Also, the accuracy of the finite-difference solution is questionable in certain regions, such as regions immediately behind the shock front, since the peak pressure is not precise, and in those regions where the density change is small. Therefore, approximate analytic solutions are desirable not only for the aforementioned reasons but also for later utilization, when the hydrodynamic theory is eventually combined with the plastic or strength-dependent theories.

Rae[3] has attempted an analytical solution based upon certain similarity assumptions, but he has not been able to obtain satisfactory results for impact problems. A few other investigators have recently tried to solve one-dimensional impact problems. Herrmann, et al.[4] have applied the finite-difference method and the stepwise characteristic method to one-dimensional low speed impact problems and have given a detailed comparison of the merits of these two numerical methods. Fowles[5] obtained an analytical expression for the decay of plane shocks by using the characteristic method. However, he neglected the entropy change across the shock front; therefore, his results are valid only for weak shocks produced by low speed impacts.

In the present report, the strong plane shock produced by hypervelocity impact is analyzed by two methods, both based on the principles of characteristics. In the first method, certain simplifying assumptions are utilized, and two approximate

analytical solutions are obtained. In the second method, a graphical stepwise characteristic approach is used. The results from these two methods demonstrate very close agreement.

The equations of state of metals used in this analysis are those obtained by Tillotson.[6] In order to facilitate the application of the characteristic method, a polynomial equation is fitted to the Hugoniot curve. Also, the isentropes are approximated by an equation similar to the one used by Murnaghan.[7]

II. Statement of the Problem

A one-dimensional plate of thickness "d", traveling at a hypervelocity, orthogonally impacts a semi-infinite plate of the same material at (x_o, t_o), (figure 1). Two shock waves are generated, one in the target and the other in the projectile. The shock wave in the projectile reaches the free boundary at (x_1, t_1), and a centered rarefaction wave reflects from this point. The head of the rarefaction wave reaches the collision boundary at (x_2, t_2) and overtakes the shock front at (x_3, t_3); from this point a continuous interaction between the rarefaction wave and the shock front ensues.

A solution to the problem involves a description of the state of the material behind the shock and an equation for the path of the shock front in the x-t plane. The solution to the above problem involves certain assumptions to insure that the problem is amenable to the fundamental hydrodynamic theory. These assumptions are developed in the text.

III. Basic Equations

The method of characteristics in fluid mechanics and the governing equations for a normal shock are well known.[8,9] In this section these basic equations are summarized for later use.

1. Normal Shock Equations

The equations expressing the conservation of mass, momentum, and energy across a shock are:

$$\rho_y (U - u_y) = \rho_x (U - u_x) \tag{1}$$

$$P_y - P_x = \rho_x (U - u_x)(u_y - u_x) \tag{2}$$

$$P_y u_y - P_x u_x = \rho_x (U - u_x)\left[E_y - E_x + \tfrac{1}{2}(u_y^2 - u_x^2)\right] \tag{3}$$

where U and u are the shock and particle velocities respectively, relative to ground (lab. coordinates); P is pressure; ρ is density; and E is the specific internal energy. Subscripts x and y refer to the states ahead of and behind the shock front respectively. The equation of state of the material may be expressed as

$$P = P(E, \rho) \tag{4}$$

If the condition ahead of the shock is known, then the quantities P_y, ρ_y, u_y, E_y and U are related by the four equations, (1) to (4). Specification of any one of these variables will determine the remaining quantities. Alternatively, if the shock Hugoniot equation

$$P = P_H(\rho) \tag{5}$$

is known, then equations (1), (2), and (5) may be used to solve for any three of the four variables P_y, ρ_y, u_y, and U, in terms of the remaining variable. In applying the method of characteristics, construction of a c,u-state plane, or a P,u-state plane is necessary. The shock condition in the p,u-plane is represented by a "shock polar", which is a curve of P_y vs. u_y, obtained from equations (1), (2), and (5). If the relationship between c and P is known, a c,u-shock polar can also be constructed.

2. Characteristic Equations

The characteristic equations for unsteady, one-dimensional, isentropic flow are

$$\frac{dx}{dt} = u \pm c \tag{6}$$

$$dp \pm \frac{\rho}{c} du = 0 \tag{7}$$

where the upper and lower signs refer respectively to the C_+ characteristics (right traveling) and the C_- characteristics (left traveling). The sound speed c is defined by

$$c^2 = \left(\frac{\partial P}{\partial \rho}\right)_s . \tag{8}$$

For isentropic flow,

$$dE = -P\,dV . \tag{9}$$

Substituting equation (9) into the general equation of state, equation (4), we obtain the isentropic P,ρ-relation (or isentrope)

$$P = P_s(\rho) . \tag{10}$$

Equations (8) and (10) may be substituted into equation (7) to yield the state characteristic equation in the c,u-state plane. The state characteristics combined with the physical characteristics, equation (6), are the basic equations for the application of the method of characteristics.

It will be shown in the next section that the isentropes used in this report have the form of equation (11).

$$P = A'\left[\left(\frac{\rho}{\rho_0}\right)^{\gamma} - 1\right] + P_0 \tag{11}$$

Equation (11) may be combined with (8) to yield

$$c^2 = \frac{A'\gamma}{\rho_0}\left(\frac{\rho}{\rho_0}\right)^{\gamma-1} = \frac{\gamma}{\rho}\left(P - P_0 + A'\right) \tag{12}$$

Equation (7) thus reduces to

$$\frac{2}{\gamma - 1}\, dc \pm du = 0 \tag{13}$$

or

$$u \pm \frac{2c}{\gamma - 1} = u_1 \pm \frac{2c_1}{\gamma - 1} \tag{14}$$

which are the equations for the state characteristics. In the c,u-plane, these characteristics are straight lines with slopes $\pm$ 2/ (γ - 1). In the P,u-state plane the characteristics are

$$u \pm \frac{2\left(\frac{A'\gamma}{\rho_0}\right)^{1/2}}{\gamma - 1}\left(\frac{P - P_0}{A'} + 1\right)^{\frac{\gamma-1}{2\gamma}} = \text{CONSTANT} \tag{15}$$

IV. Equation of State

For the present problem, the pressure in the solid material is of the order of 1/10 to 10 megabars. Under a pressure of this magnitude, the strength effect and the deviatoric components of stress can be neglected. One equation relating three state properties is sufficient to describe the state of the material. In other words, the material behaves like an ideal compressible fluid, and the equation of state is similar to that used in hydrodynamics.

Under this hydrodynamic assumption, Tillotson obtained the following equation of state which is accurate for a large pressure range, (equation (6) ref. 9).

$$P = \left[a + \frac{b}{\frac{E}{E_o \eta^2} + 1} \right] \frac{E}{V} + A\mu + B\mu^2 \qquad (16)$$

where P= the pressure in megabars

E= specific internal energy in megabars-cm^3/g

V= $1/\rho$ specific volume in cm^3/g

$\eta = \rho/\rho_o = V_o/V$, where ρ_o is normal density, and

$\mu = \eta - 1$

and a, b, A, B, E_o are constants dependent upon the metal. This equation is semi-empirical in nature and represents a best-fit extrapolation between Thomas-Fermi-Dirac data at high pressures (above 50 megabars) and shock wave experimental data at low pressures. This equation is accurate to approximately 5% of the Hugoniot pressure and 8% of the isentropic pressure.

Equation (16) is simple in form and is convenient for numerical calculation of hypervelocity impact problems by the finite-difference methods. However, it is not suitable to obtain an analytical solution to the present problem by the characteristic method. A further simplification is incorporated by fitting simple equations to the Hugoniot and isentropes of equation (16).

Table I contains data for aluminum which is calculated from the equation of state, equation (16), and the normal shock conditions. (See Appendix A). Two approaches have been used to fit the Hugoniot data in Table I. In the first approach, the Hugoniot is represented by a curve of U vs. Z, where Z= u+c. This curve is fitted by the following equation.

$$U = a_1 + b_1 Z + c_1 Z^2 \tag{17}$$

where the constants a_1, b_1, and c_1 are obtained by the method of least squares. Figure 2b gives a comparison of equation (17) with the data in Table I. The error is found to be less than 0.6 % for a range of 1 to 10 megabars. In the second approach, an equation relating U and u,

$$U = a_2 + b_2 u + c_2 u^2 \tag{18}$$

is obtained by the method of least squares. Figure 2a compares equation (18) with the data in Table I. The accuracy of this equation is within 2% for a pressure of 1 to 10 megabars. Two different analytical solutions for the shock path are developed in Section V,#3, by using equations (17) and (18), respectively.

For the isentropes, an equation similar to Murnaghan's is assumed,

$$P = A' \left[\left(\frac{\rho}{\rho_o} \right)^{\gamma} - 1 \right] + P_o \tag{11}$$

From each point on the P-v Hugoniot curve, an isentrope may be calculated from equation (16). Equation (11) is fitted to those isentropes, and the constants A', γ and P_o are determined; each of these constants assumes a different value for every isentrope. Table I gives values of these constants for aluminum. The accuracy of equation (11) as compared to equation (16) is very good as shown in figure 3.

In the present report, the Hugoniot and isentrope equations are fitted to data presented in Ref. 6. Actually, Hugoniots of the form of equation (17) and (18) and isentropes of the form of equation (11) generally can be fitted to other equations of state data, theoretical or experimental.

V. Analytical Solutions

1. Assumptions

Besides the assumptions of a hydrodynamic equation of state and an adiabatic, non-viscous process, additional assumptions are required to obtain an analytical solution for the decay of strong shocks. Fowles[5] assumed that the change of the entropy across the shock front is negligible, and thus his solution is limited to weak shocks. For strong shocks, however, the entropy change across the shock is appreciable and cannot be neglected.

Behind a strong shock the characteristic lines, to be exact, are not straight lines. However, the interactions between C_+ and C_- characteristics and between characteristics and contact lines are usually weak. In the present analytical approach, we assume that the characteristic lines in the rarefaction wave originating from point (x_1, t_1), figure 1, remain straight. Furthermore, either the particle velocity u, or the sum of particle velocity and sound speed u + c, is assumed constant along any one of these characteristic lines.

These assumptions are similar to those used in reference 10, which treats the decay of plane strong shocks in an ideal gas. The assumption of characteristic lines remaining straight has also been used by Al'tshuler, et al.[11] in an experimental technique to determine the sound velocity behind a strong shock. Although the details are not given in their paper, they have also performed numerical calculations to show that the error involved in their assumption of straight characteristic lines is small.

If the values of u are assumed constant along characteristic lines behind the shock front, the path of the shock can be determined from the exact shock equations. For points directly behind the shock front, the sound speed calculated from the exact shock equation is different from the sound speed on the same

straight characteristic line near point (x_1,t_1). In the region immediately behind the shock front, therefore, this approach results in an inconsistency in sound speed, and consequently in pressure. The sound speed and pressure calculated from the shock equation are taken as the correct value behind the shock, and a linear variation in properties between the shock front and the rarefaction tail is assumed.

In the approach of u + c= constant, the values of u and c singly are not assumed constant along the straight characteristic lines. The values of c and u behind the shock front are determined by the shock conditions, while a linear variation for these quantities is assumed between the shock and the tail of the rarefaction wave.

2. Initial Conditions

According to equations (1) and (2), the shocks in the target and the projectile, immediately after impact, are governed by the conditions

$$\left.\begin{aligned} \rho_1 U_T &= \rho_2 (U_T - u_2) \\ P_2 - P_1 &= \rho_1 (U_T u_2) \end{aligned}\right\} \text{TARGET} \qquad (19), (20)$$

$$\left.\begin{aligned} \rho_0 (U_P - u_0) &= \rho_2 (U_P - u_2) \\ P_2 - P_0 &= \rho_0 (U_P - u_0)(u_2 - u_0) \end{aligned}\right\} \text{PROJECTILE.} \qquad (21), (22)$$

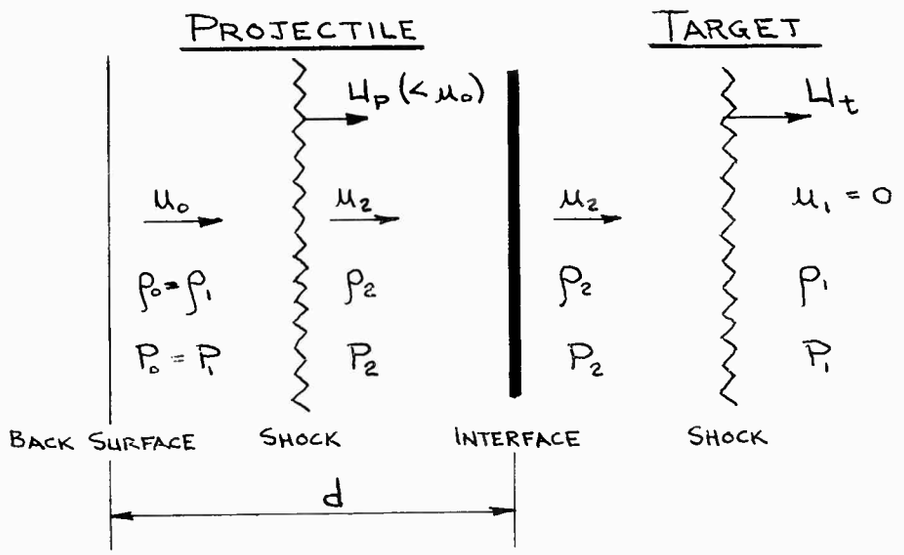

FIGURE a.
Initial Shock Configuration

where the subscripts refer to regions in figure a, and all velocities are relative to the ground (positive toward the right). Solving equations (19) to (22), we obtain the following relation

$$U_t = -(U_p - u_o) \quad (23)$$

This equation indicates that impact between similar materials yields shock velocities (relative to the material ahead) in both the target and the projectile, with equal magnitude but opposite signs.

Equation (23) may be substituted into equations (21) and (22) to yield

$$\rho_1 U_t = \rho_2 (U_T - u_o + u_2) \quad (24)$$

$$P_2 - P_1 = \rho_1 U_t (u_o - u_2) \quad (25)$$

equations (20) and (25) gives

$$u_2 = \frac{1}{2} u_o \quad (26)$$

Since U_t equals the magnitude of the shock velocity relative to the projectile, the time required for the shock in the projectile to reach the free boundary is

$$t_1 - t_o = \frac{d}{U_t} \quad . \tag{27}$$

The absolute velocity of the shock in the projectile is $U_p = - U_T + \mu_o$; therefore

$$x_1 - x_o = (t_1 - t_o)(-U_t + \mu_o) \quad . \tag{28}$$

By combining equations (19), (20), (26), (27) and (28), and using the geometry of the x,t-plane, we find that the head of the rarefaction wave reaches the collision boundary at time t_2 given by

$$t_2 - t_1 = (\rho_1 d)/(\rho_2 c_2) \quad . \tag{29}$$

The interaction between the rarefaction wave and the shock front in the target starts at time t_3, which is given by

$$t_3 - t_2 = \frac{x_3 - x_2}{\mu_2 + c_2} = \frac{(t_3 - t_o)U_t - \mu_2(t_2 - t_o)}{\mu_2 + c_2} \quad . \tag{30}$$

After simplification, equation (30) can be written as follows

$$t_3 - t_o = \frac{c_2 (t_2 - t_o)}{\mu_2 + c_2 - U_t} \quad . \tag{31}$$

From (27) and (29), we obtain

$$t_2 - t_o = (t_2 - t_1) + (t_1 - t_o) = \frac{\rho_1 d}{\rho_2 c_2} + \frac{d}{U_t} \quad . \tag{32}$$

Substitution for $(t_2 - t_o)$ from (32) in (31) yields

$$t_3 - t_o = \frac{c_2 d}{\mu_2 + c_2 - U_t}\left[\frac{\rho_1}{\rho_2 c_2} + \frac{1}{U_t}\right] \quad . \tag{33}$$

The distance traveled by the shock before it is overtaken by the rarefaction wave is given by

$$X_3 - X_0 = (t_3 - t_0)U_t = \frac{U_t C_2 d}{u_2 + C_2 - U_t}\left[\frac{\rho_1}{\rho_2 C_2} + \frac{1}{U_t}\right] . \quad (34)$$

Up to the point (x_3, t_3), the shock front is a straight line. From this point on the shock front becomes a curved line and the shock strength attenuates.

3. Attenuation of the Shock

The study of shock attenuation is attempted by two approaches . In the first approach, the characteristic lines in the x,t-plane are assumed as straight lines, and along each characteristic the sum of the particle and sound velocities is assumed constant. In the second approach, the (x,t) characteristic lines are again considered straight, but now only the particle velocity along each characteristic line is assumed constant. The two approaches are given below.

a) "u+c= constant" Approach

A centered rarefaction wave starts at the point (x_1, t_1). Since the characteristic lines are assumed to be straight, the equation of a characteristic line originating from this point is

$$x - x_1 = (u + c)(t - t_1) . \quad (35)$$

After substituting $u + c = Z$, equation (35) becomes

$$x - x_1 = Z(t - t_1) . \quad (36)$$

Differentiating both sides of equation (36) with respect to Z, we obtain

$$\frac{dx}{dZ} = (t - t_1) + Z\frac{dt}{dZ} . \quad (37)$$

Also, along the shock path

$$\frac{dx}{dz} = \frac{dx}{dt} \cdot \frac{dt}{dz} = U \frac{dt}{dz} \tag{38}$$

where U is the shock propagation velocity.

From equations (37) and (38) we see that

$$U \frac{dt}{dz} = (t - t_1) + z \frac{dt}{dz} \cdot \tag{39}$$

Substituting the expression for U in terms of Z, equation (17), into equation (39), integrating and simplifying the resulting equation, we obtain

$$t = t_1 + (t_3 - t_1)\left[\frac{\alpha + z}{\alpha + z_2} \cdot \frac{\beta + z_2}{\beta + z}\right]^{D/c_1} \tag{40}$$

where

$$\alpha = \frac{1}{2}\left[\sqrt{\left(\frac{b_1 - 1}{c_1}\right)^2 - \frac{4a_1}{c_1}} + \frac{(b_1 - 1)}{c_1}\right]$$

$$\beta = \frac{-1}{2}\left[\sqrt{\left(\frac{b_1 - 1}{c_1}\right)^2 - \frac{4a_1}{c_1}} - \frac{(b_1 - 1)}{c_1}\right]$$

and

$$D = \frac{1}{\beta - \alpha} \cdot$$

Equations (36) and (40) define the desired shock path in parametric form with Z as the parameter and t_1, t_3, and x_1 as constants, (figure 1), and Z_2 is also a constant which is equal to the sum of the particle velocity and the sound velocity behind the shock immediately after impact.

b) "u= constant" Approach

Following the manner of the previous section, the equation of a characteristic line starting from the point (x_1, t_1) can be written as

$$x - x_1 = (u + c)(t - t_1) \quad (41)$$

Also, for a characteristic line, according to equation (14)

$$u - \frac{2c}{\gamma - 1} = u_2 - \frac{2c_2}{\gamma - 1} \quad (42)$$

The constant γ depends on the pressure behind the shock (see Appendix A).

Defining ℓ_1 as

$$\ell_1 = -\left(u_2 - \frac{2c_2}{\gamma - 1}\right) \quad (43)$$

we may rewrite equation (42) as

$$c = \frac{\gamma - 1}{2}(u + \ell_1)$$

Thus, from equation (41),

$$x - x_1 = \left(\frac{\gamma + 1}{2} u + \frac{\gamma - 1}{2} \ell_1\right)(t - t_1) \quad (44)$$

Differentiating both sides of equation (44) with respect to u, we obtain

$$\frac{dx}{du} = \frac{dx}{dt}\frac{dt}{du} = \frac{\gamma + 1}{2}(t - t_1) + \left(\frac{\gamma + 1}{2} u + \frac{\gamma - 1}{2} \ell_1\right)\frac{dt}{du} \quad (45)$$

Substituting equation (18) into equation (45), with $U = \frac{dx}{dt}$, we obtain

$$(a_2 + b_2 u + c_2 u^2)\frac{dt}{du} = \frac{\gamma + 1}{2}(t - t_1) + \left(\frac{\gamma + 1}{2} u + \frac{\gamma - 1}{2} \ell_1\right)\frac{dt}{du} \quad (46)$$

or

$$\frac{dt}{t - t_1} = \frac{\gamma + 1}{2} \frac{du}{c_2 u^2 + e_2 u + d_2} \quad (47)$$

where

$$e_2 = b_2 - \frac{\gamma+1}{2} \quad , \tag{48}$$

$$d_2 = a_2 - \frac{\gamma-1}{2} l_1 \quad . \tag{49}$$

Integrating both sides of equation (47), we obtain

$$t = t_1 + (t_3 - t_1)\left[\frac{2c_2 u + e_2 - \sqrt{e_2^2 - 4c_2 d_2}}{2c_2 u + e_2 + \sqrt{e_2^2 - 4c_2 d_2}} \cdot \frac{2c_2 u_2 + e_2 + \sqrt{e_2^2 - 4c_2 d_2}}{2c_2 u_2 + e_2 - \sqrt{e_2^2 - 4c_2 d_2}}\right]^K ,$$

$$\text{WHERE } K = \frac{\gamma+1}{2(e_2^2 - 4c_2 d_2)^{1/2}} \tag{50}$$

Equations (50) and (44) represent the shock path in a parametric form, where u is the parameter.

4. Fowles' Solution

Fowles' weak shock solution is given below for the purpose of comparison. His equations for the path of the shock front are

$$t(\sigma) = t_1 + (t_3 - t_1)\left[\frac{\sigma_0}{\sigma_0 - 2(\gamma'+1)}\right]^2 \left[\frac{\sigma - 2(\gamma'+1)}{\sigma}\right]^2 \quad (t > t_3) \tag{51}$$

and

$$x(\sigma) = x_1 + c_1(\sigma+1)(t_3 - t_1)\left[\frac{\sigma_0}{\sigma_0 - 2(\gamma'+1)}\right]^2 \left[\frac{\sigma - 2(\gamma'+1)}{\sigma}\right]^2 \quad (t > t_3) \tag{52}$$

where γ' = a constant depending on the material (4.266 for aluminum),

$$\sigma = \frac{u + c}{c_1} - 1$$

and

$$\sigma_0 = \frac{x_3 - x_1}{c_1(t_3 - t_1)} - 1 \quad .$$

He used equation (11) with one set of constants as both the isentrope and the Hugoniot for calculating the initial conditions.

VI. Graphical Solutions

1. General Discussion

The graphical solution of the present problem is obtained by the "field method" of stepwise characteristics. Although this method is time consuming, it yields a very accurate solution which may be used as a basis of comparison for the approximate analytical solutions.

The complete solution involves the determination of the path of the shock front and a description of the physical properties of the material behind the shock. This solution is achieved through the use of three planes, the physical plane ($c_o t, x$-diagram of figure 4), the P,u-state plane (figure 5a) and the c,u-state plane (figure 5b). A region of continuously varying fluid properties in the physical plane is replaced by a number of finite regions each having uniform fluid properties. These regions are divided by characteristic or contact lines, across which the properties change. The complete solution requires the use of shock polars and characteristics in the c,u and P,u state planes.

In the present problem, only one shock polar is required. This shock polar is plotted in both state planes from the data given in Table 1. The origin of the shock polar represents conditions in the target preceding impact, i.e., $u = 0$, $P = 0$ and $c = 5.275$ km/sec.

Equation (14), in the following form, is used to plot the c,u-characteristics

$$\left[u \pm \frac{2c}{\gamma - 1} = u_H \pm \frac{2c_H}{\gamma - 1} \right]_{I,II} \tag{14}$$

where c_H and u_H are the properties in the region immediately behind the shock. In the c,u-state plane the characteristics are straight lines with slopes equal to

$$\left[\frac{dc}{du} = \mp\frac{\gamma-1}{2}\right]_{I,II}$$

where γ is a constant for a particular isentrope which is found in Table I with u_H equal to u.

Equations 11, 12, and 14 are combined to yield the P,u-characteristics

$$\left[u \pm \frac{2}{\gamma-1}\left(\frac{A'\gamma}{\rho_o}\right)^{1/2}\left(\frac{P-P_o}{A'}+1\right)^{\frac{\gamma-1}{2\gamma}} = u_H \pm \frac{2c_H}{\gamma-1}\right]_{I,II} \quad (15.a)$$

where $u_H \pm \frac{2C_H}{\gamma-1}$ is a constant and depends upon the properties of the region behind the shock. The constants A', γ, P_o and c_H may also be obtained from Table I.

The P,u-state plane is required in the graphical solution because it yields a simpler solution for the physical properties in the regions bounding the contact lines. These regions have identical pressures and particle velocities and therefore plot as a single point in this plane. The c,u-state plane yields the required sound velocity to construct the physical (c_1t-x) diagram.

2. Detailed Procedure

The graphical solution is obtained by constructing the complete flow field in the physical and state planes. Figure 1 schematically illustrates the physical plane. At the point of impact (x_o, t_o) two shocks originate. The initial position of the right traveling shock can be constructed with the slope c_1/U_T. The left traveling shock is constructed with the slope $\frac{c_1}{U_p}$. The slopes of the physical characteristics are given by

$$\left[\frac{d(c,t)}{dx} = \frac{C_1}{u \pm C}\right]_{I,II}$$

where the upper sign refers to the I-characteristic (C_+ or right-traveling waves) and the lower sign refers to the II-characteristics (C_- or left-traveling waves). Both the sound velocity c and particle velocity u represent the average between their respective values on both sides of the characteristic line.

The simple rarefaction wave centered at (c_1t_1, x_1) is arbitrarily divided into six regions by assuming approximately equal increments of particle velocity between adjacent regions. These waves are propagated with constant strength until the head of the rarefaction wave overtakes the shock front. An interaction between the waves and the shock front then follows. As the shock continues with both decreased strength and velocity, contact lines and reflected waves are formed. A contact line, which separates regions of unequal entropy, forms because the fluid particles passing through shocks of unequal strength attain different levels of entropy. A reflected wave is required in order to satisfy the boundary conditions of equal pressure and equal particle velocity across a contact line. All the regions bounded by the shock path and a pair of neighboring contact lines are at the same entropy level: therefore the coefficients A', γ and P_o which are used in the characteristic equations are constant within each of these regions. When crossing a contact line, new values for A', γ and P_o must be selected from Table I.

The properties of regions 1 and 2 are determined by the initial conditions of the problem. From the assumed particle velocities in regions 3 to 9, the pressures and sound velocities can be determined by the method of characteristics. Regions on both sides of a contact line have equal pressures and particle velocities, (i.e., the pressure and particle velocity in regions 10 and 20 are equal). Therefore the points 10' and 20' in the P-u state plane coincide. In the

c,u-plane, figure 5, point 10 lies directly above point 20. Similarly, regions 21 and 30 plot as a single point in the P,u-state plane and lie at the intersection of a I-characteristic through point 11 and a II-characteristic through point 20.

For a complete and detailed discussion of the graphical method of solution, the reader is referred to references 8, 9, and 10.

As an example of the graphical method applied to the present problem, an impact velocity of 28.2 km/sec was chosen. Figure 4 shows the physical plane and Table II gives the physical properties in selected regions.

VII. Comparison of Results

In this section the accuracy and the results of the two analytical approaches will be compared with each other. The analytical results will then be compared with the graphical solution and Fowles' solution. The paths of the shock as obtained by the two analytical approaches, "u=constant" and "u+c= constant", are shown in figure 7. For small values of time the two assumptions yield identical paths; for large values of time, the paths diverge progressively. The relative accuracy of these two approaches can be evaluated from the c,u-state plane in the graphical solution as shown schematically in figure 8a. Numbered points in this figure refer to regions in figure 4. The exact properties in regions 2, 4, and 20 as determined by the graphical method are represented by the points 2, 4, and 20, respectively, in figure 8a. According to the "u=constant" approach, the particle velocity in region 20, u_{20}, is equal to that in region 4, u_4. Therefore, the properties in region 20 are represented in figure 8 by point 20': the intersection of the vertical line through point 4 and the shock polar. According to the "u+c= constant" approach

$$u_{20} + C_{20} = u_4 + C_4 . \tag{53}$$

Thus region 20 is represented in figure 8a by point 20": the intersection of the straight line plotted from equation (53) and the shock polar. (Equation (53) is a straight line inclined at 45° from the axes if c and u are plotted in the same scale). An inspection of figure 8a shows that point 20" is much closer to point 20 than is point 20'. A similar discussion can also be made for points 5, 70, 70', and 70". The "u+c=constant" approach can be expected, therefore, to be more accurate than the "u=constant" approach.

Another way of evaluating the relative accuracy of these two approaches is to compare the change in u and u+c between two regions, one immediately

behind the shock and one in the simple wave region, such as regions 20 and 4 or regions 70 and 5, in figure 4. Table 3a shows the results of such a comparison. Again, it can be seen that "u+c" changes less than "u", and "u+c= constant" is a better approximation.

The discussion in the preceding paragraphs is true for aluminum. No conclusion has been reached for metals in general. It is interesting to note that calculations made for an ideal gas with a ratio of specific heat of 1.4 indicate an opposite trend. That is, the "u=constant" approach is more accurate than the "u+c= constant" approach, as demonstrated by figure 8b and Table 3b. Figure 8b is constructed in the same manner as figure 8a and with the points similarly numbered. The major difference between the two is that for the ideal gas, figure 8b, the shock polar is below the II-characteristic line in the region of points 2, 4, and 5. Primarily due to this change in the relative position of the shock polar and characteristic, the trend in the accuracy of the two approaches is reversed. Table 3b is calculated in the same manner as Table 3a. The equivalent impact velocity used for the ideal gas is 1.22 km/sec, and the ratio of specific heat is taken as 1.4.

For weak shocks, the paths of the decaying shock obtained from all three methods (analytical, graphical and Fowles') fall on one curve. For strong shocks, the present analytical solution is in close agreement with the graphical solution, whereas Fowles' solution deviates considerably from the other two, as shown in figure 6.

VIII. NOTATIONS

c	-	sound speed
d	-	thickness of projectile
E	-	specific internal energy
P	-	pressure
t	-	time
u	-	particle velocity
U	-	shock velocity
V	-	specific volume
x	-	distance
Z	-	u+c sum of particle velocity and sound speed
ρ	-	density
γ, A'	-	parameters in the equation of the isentropes

SUBSCRIPTS

ρ_o	-	density at atmospheric conditions
P_o	-	pressure on an isentrope where $\rho_o/\rho = 1$
U_p	-	shock velocity in projectile (relative to ground)
U_t	-	shock velocity in target (relative to ground)
$( )_o$	-	undisturbed region in projectile
$( )_1$	-	undisturbed region in target
$( )_2$	-	region behind shocks (immediately after impact)
$( )_s$	-	constant entropy
$( )_H$	-	regions behind shocks or points on Hugoniot

subscripted x or t refers to figure 1

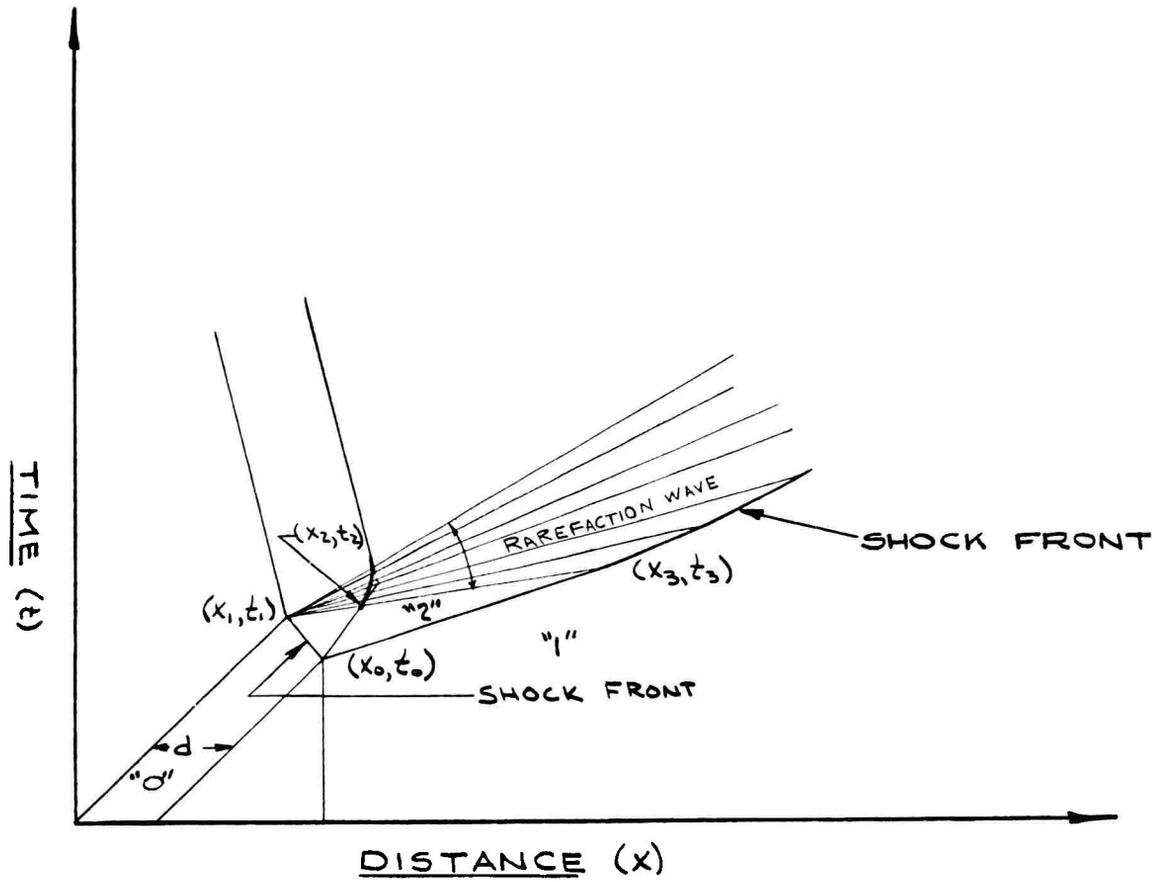

Figure 1. Plane Shock Due to Impact, Physical Plane (Schematic)

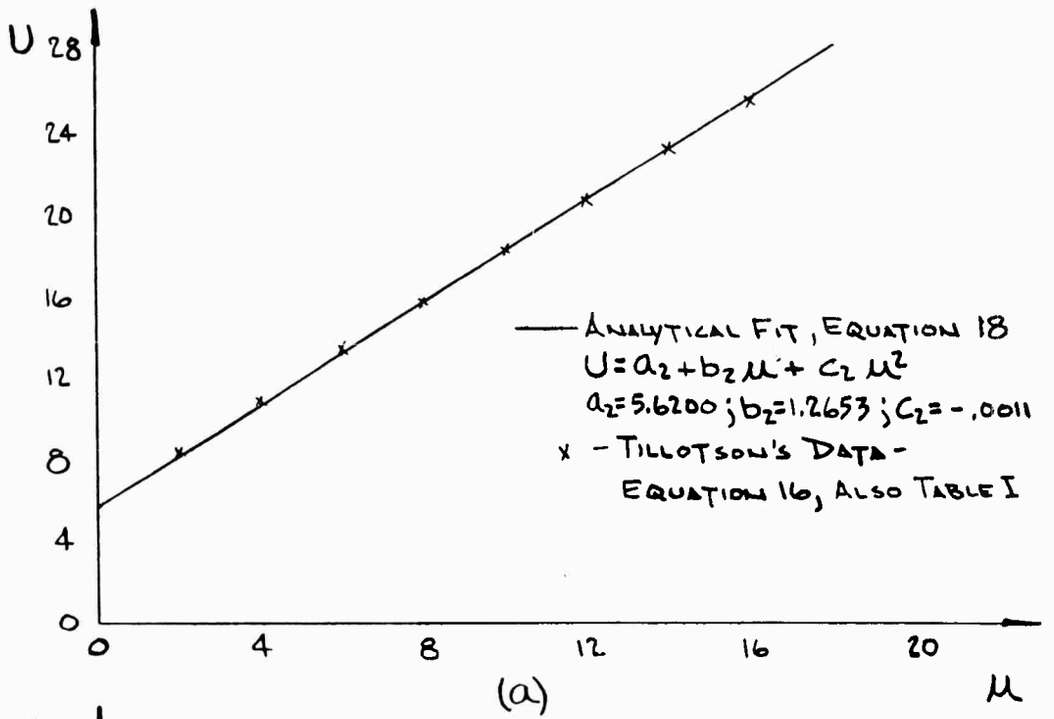

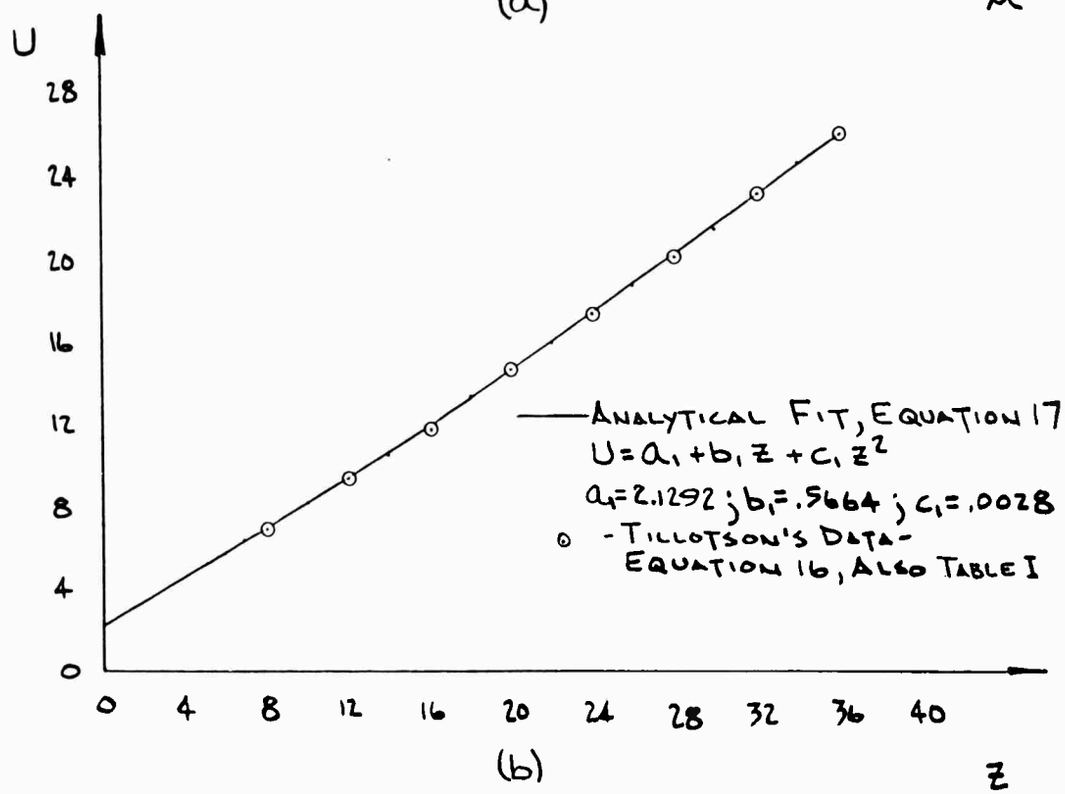

Figure 2. Comparison of the Fitted Equations with Tillotson's Data
(a) $U = a_2 + b_2 \mu + c_2 \mu^2$
(b) $U = a_1 + b_1 Z + c_1 Z^2$

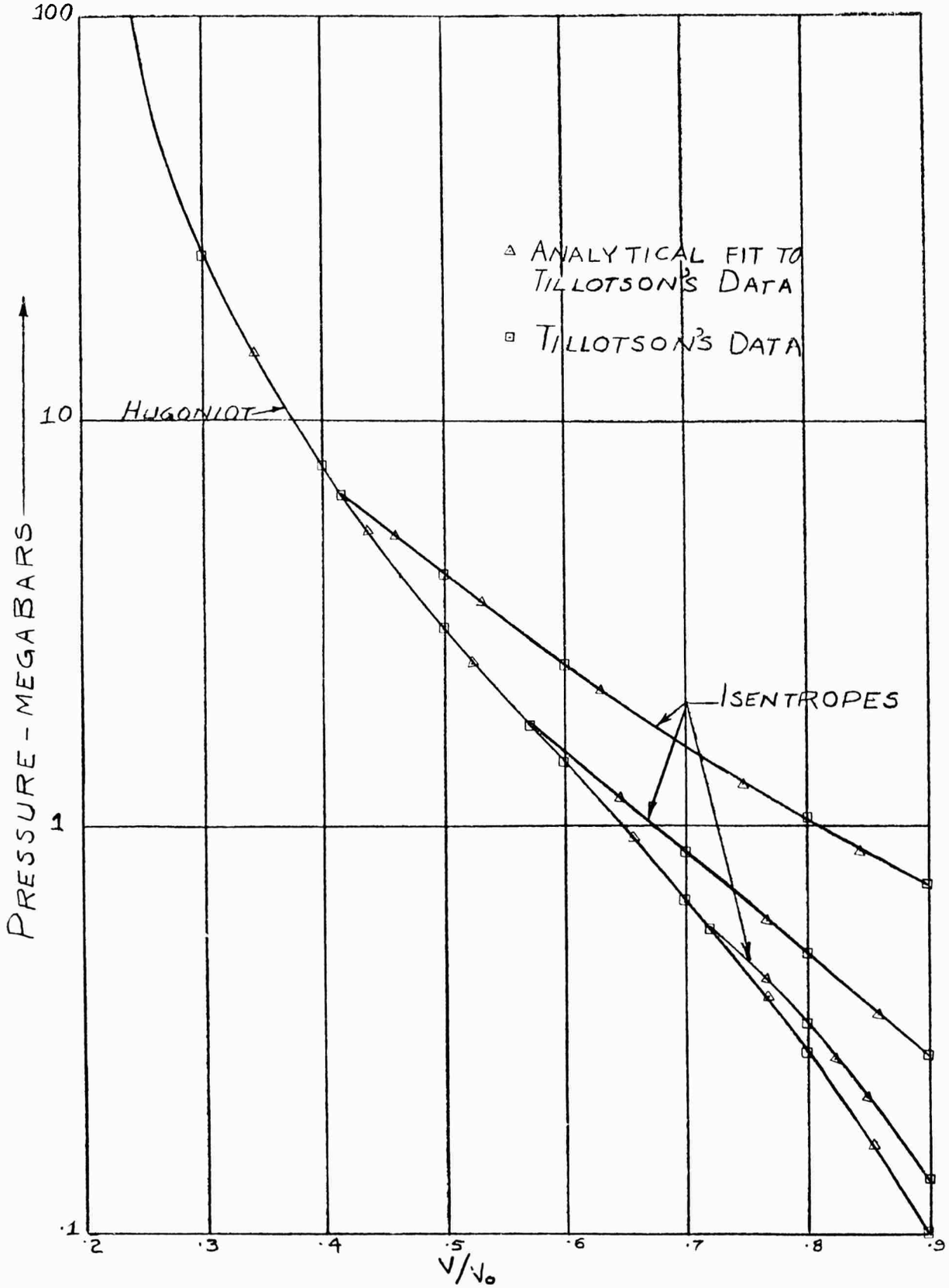

Figure 3. Equation of State for Aluminum

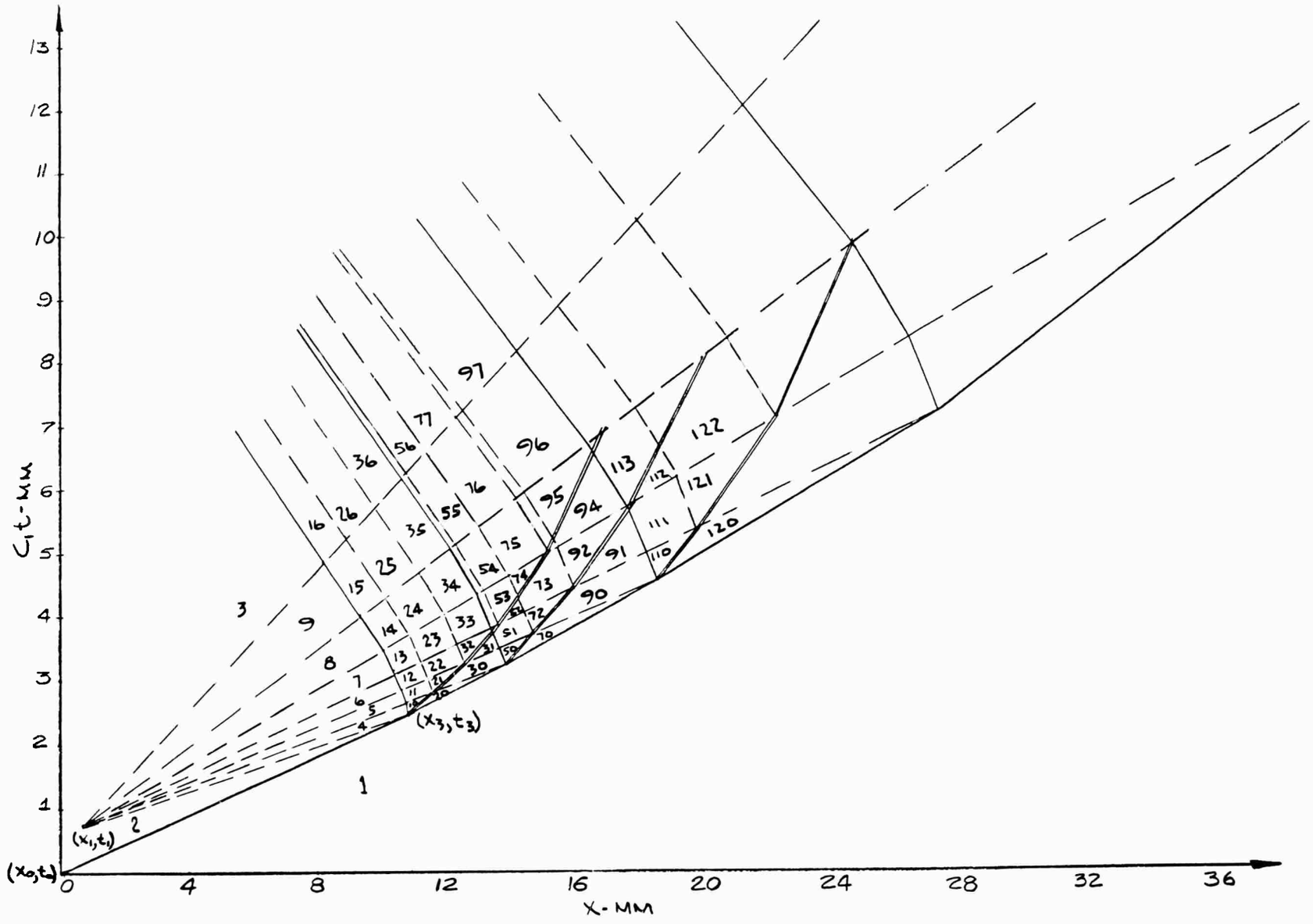

Figure 4. Regions in the Physical Plane Used in the Stepwise-Graphical Characteristics Method

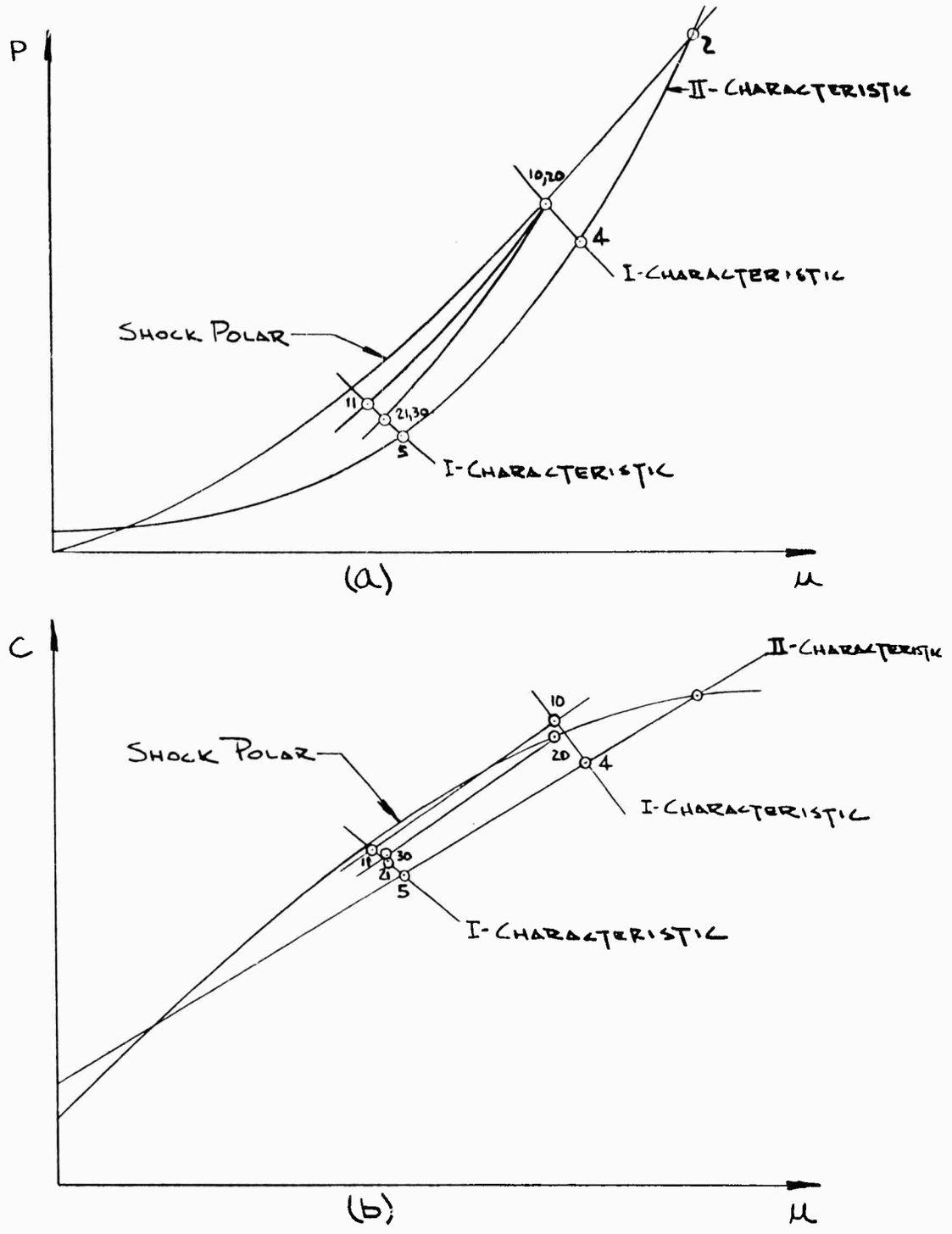

Figure 5 - State Planes (Schematic)
(a) P versus u State Plane
(b) c versus u State Plane

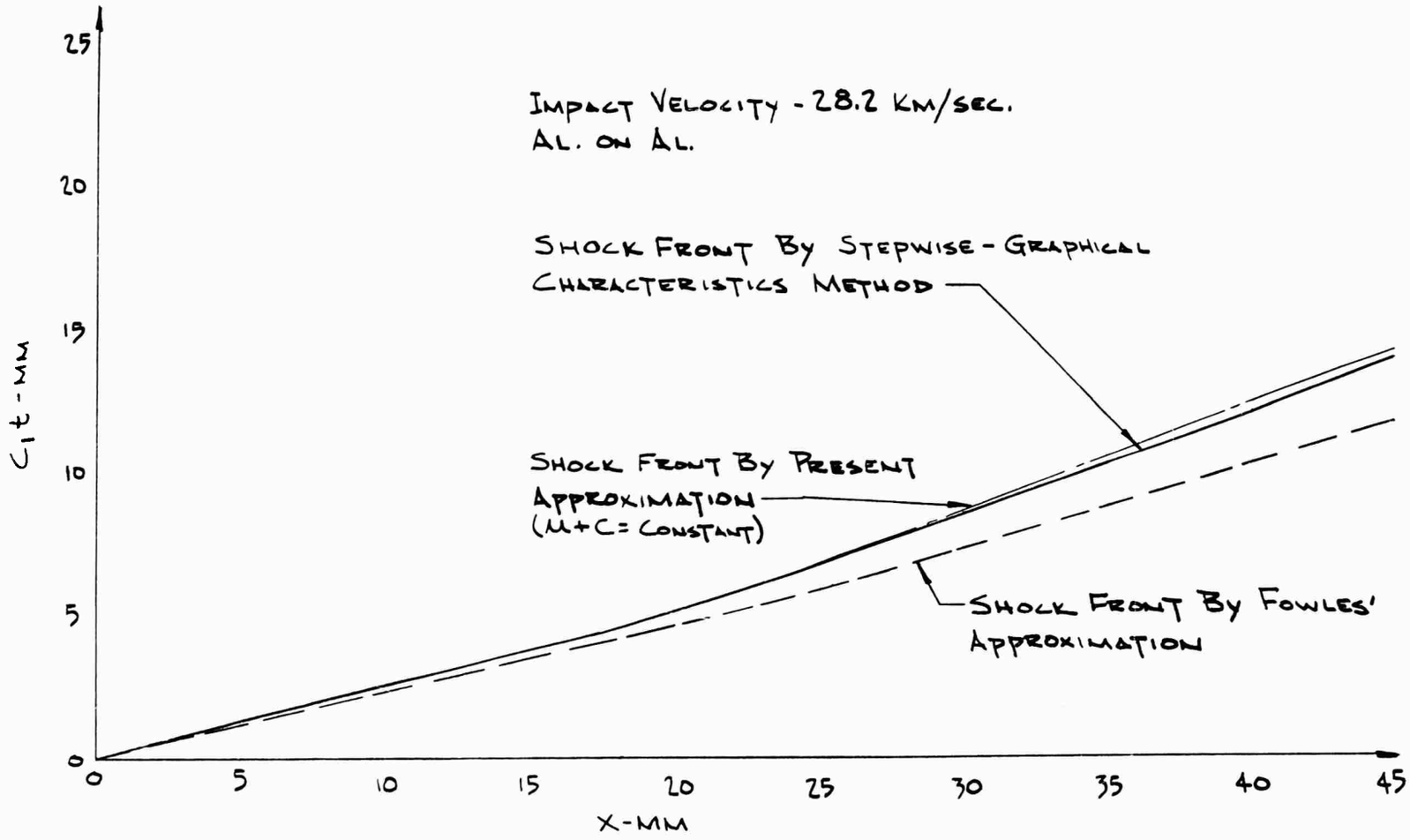

Figure 6 a. Position of Shock Front by Different Methods (Small times)

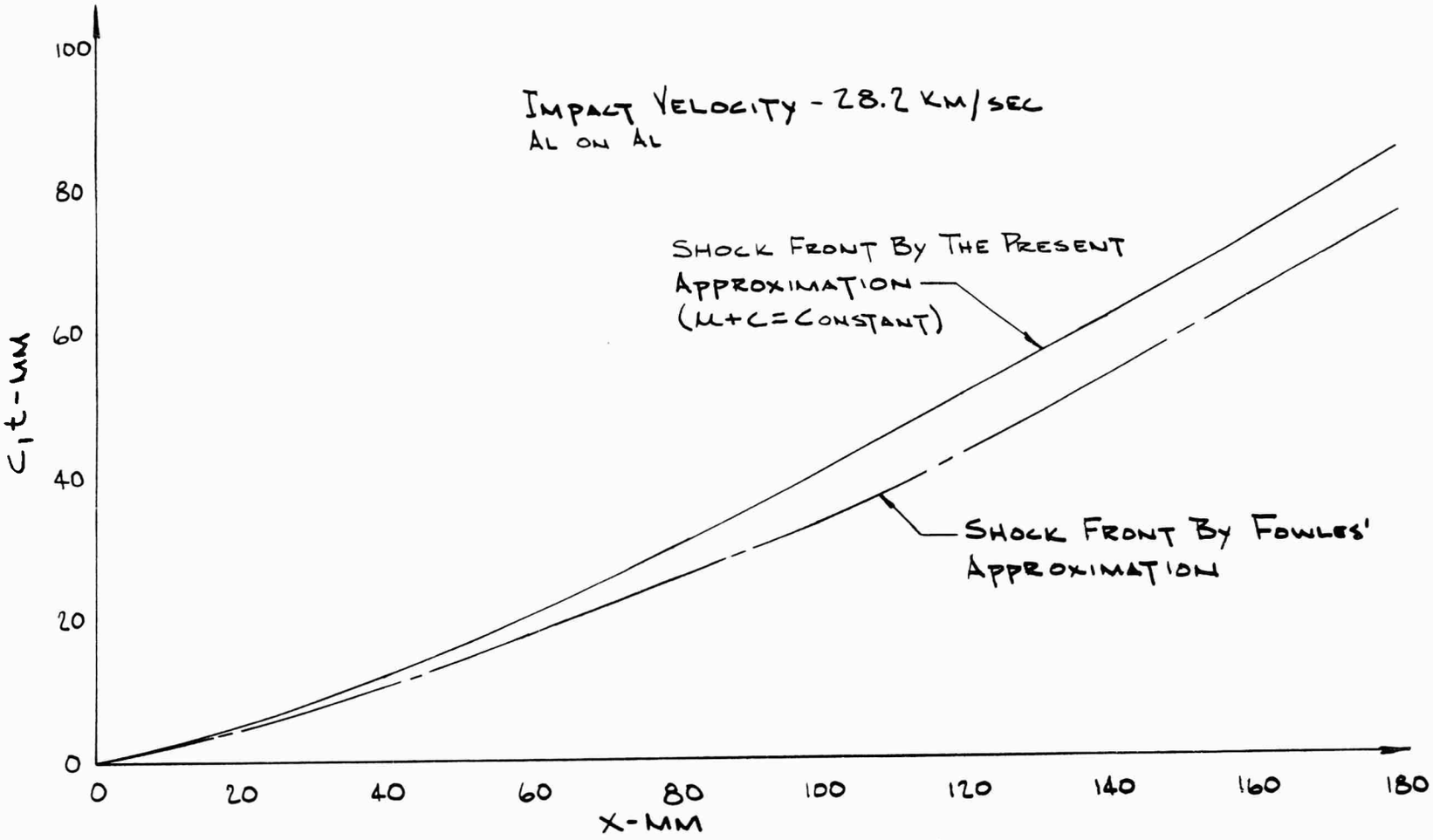

Figure 6b. Position of Shock Front by Different Methods (Large times)

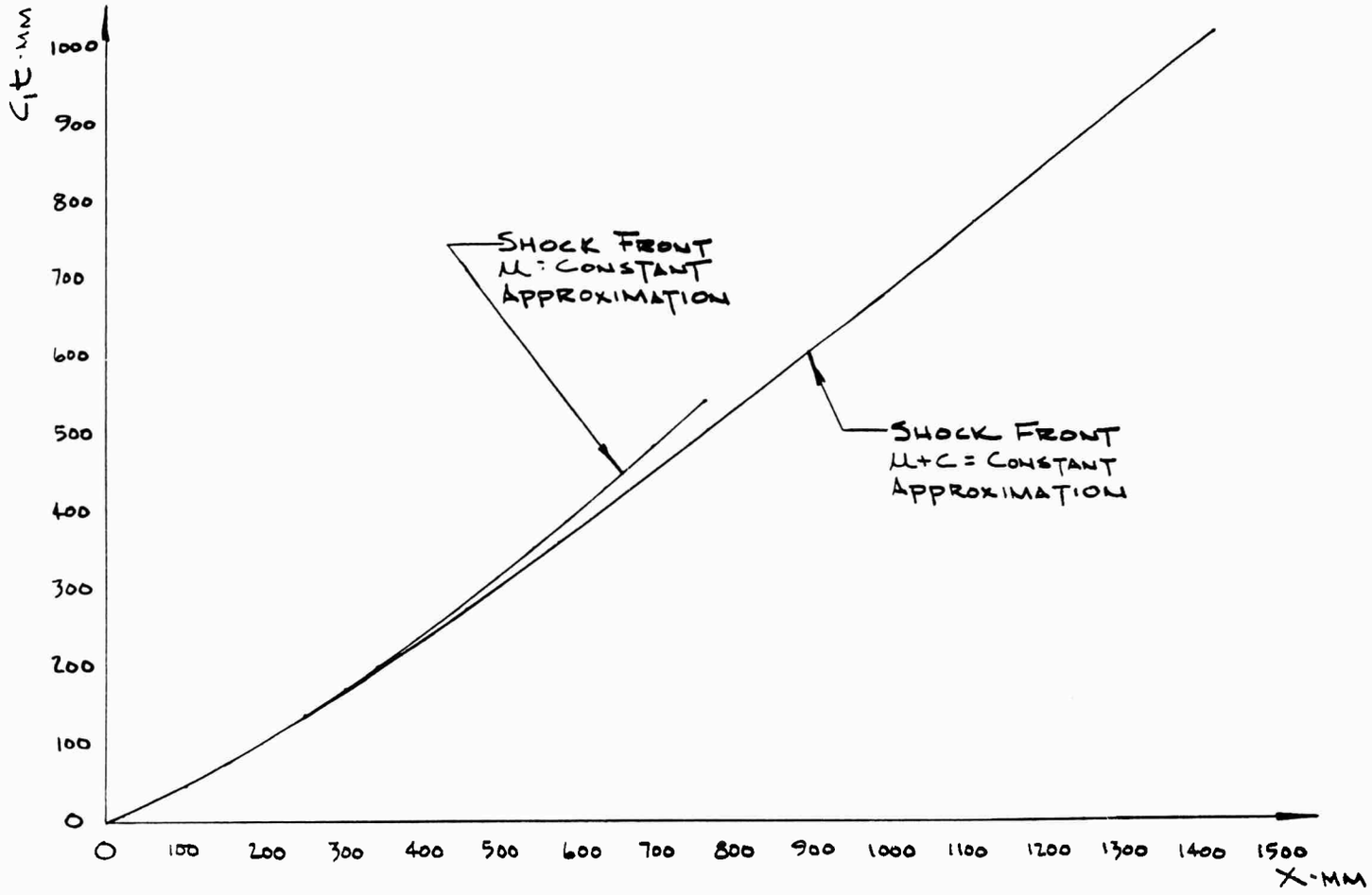

Figure 7. Position of Shock Front by Present Approximations (u + c = constant, u = constant)

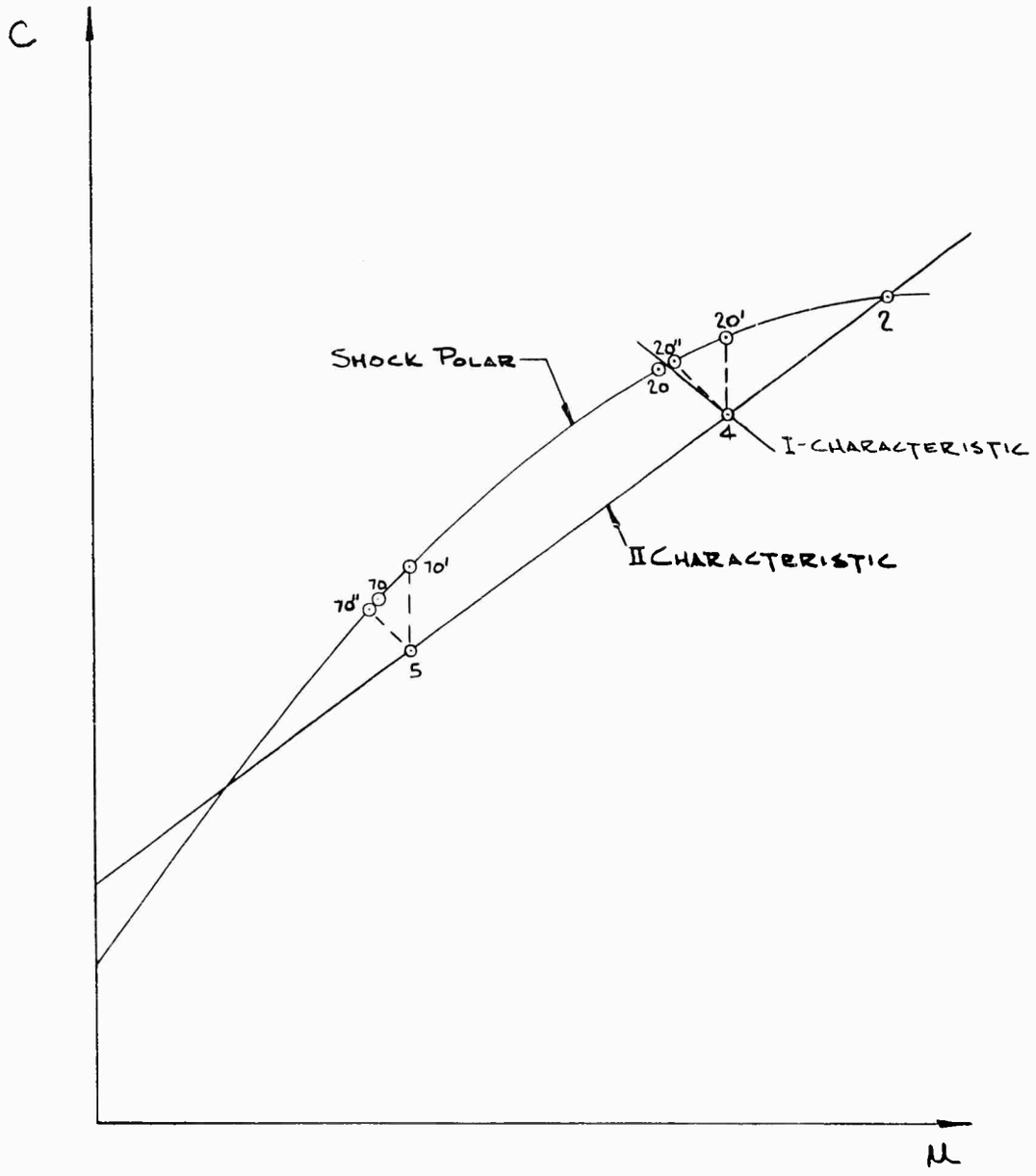

Figure 8a. Schematic Illustrating the Relative Accuracy of the u = constant Assumption and u + c = constant Assumption for Aluminum.

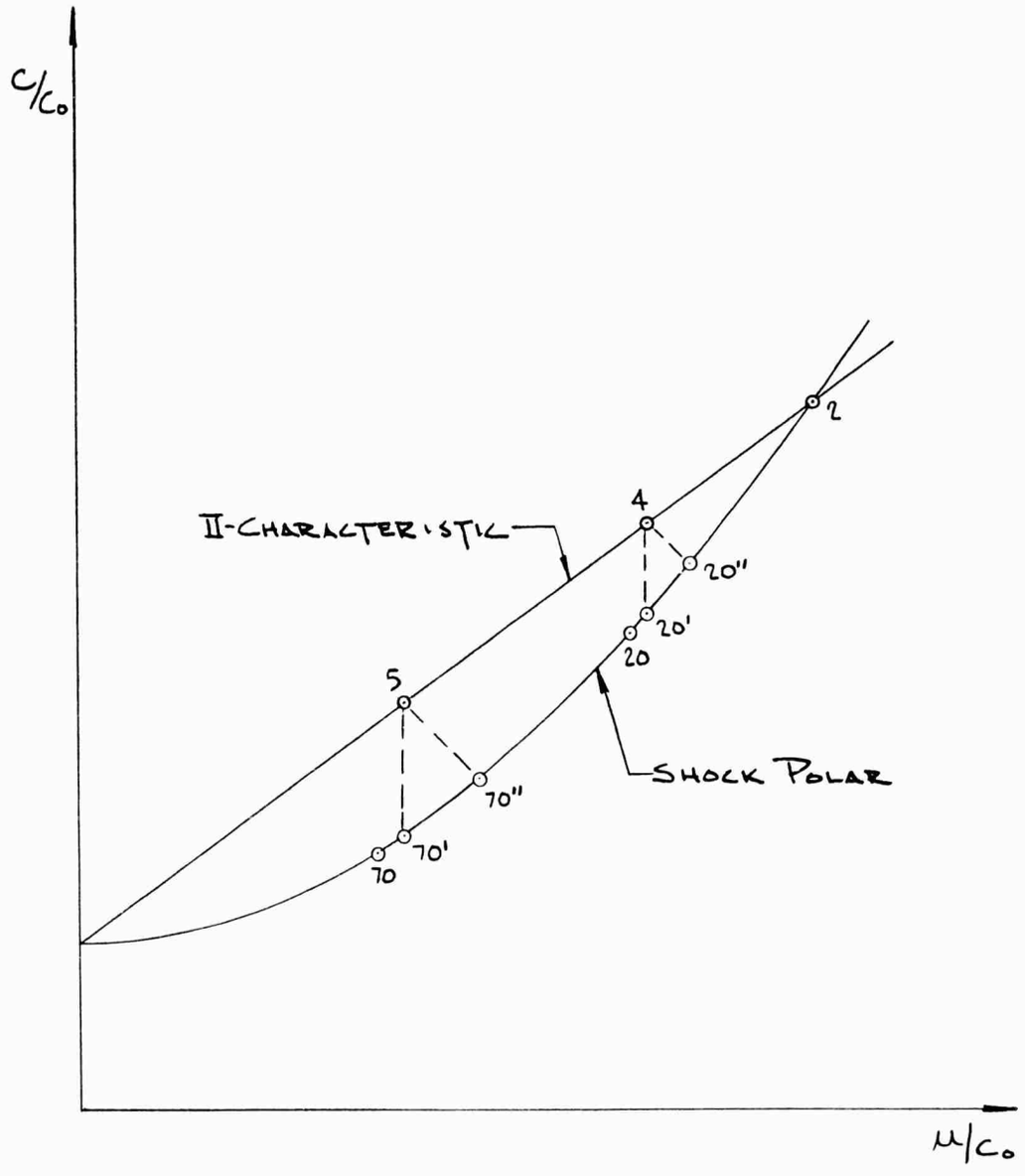

Figure 8b. Schematic Illustrating the Relative Accuracy of the u = constant Assumption and u + c = constant. Assumption for Ideal Gas.

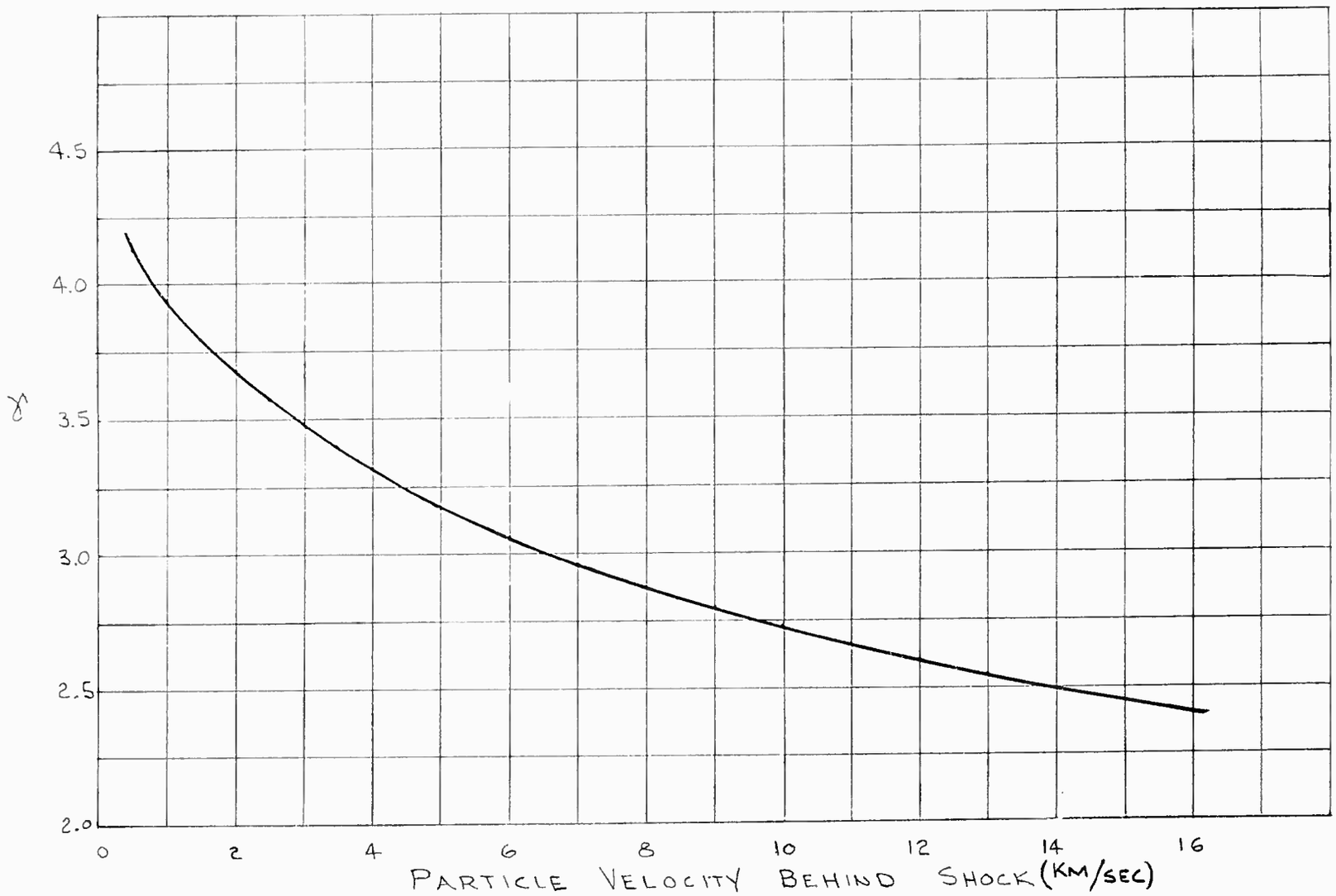

Figure 9. Constants in Isentrope Equation 11 for Aluminum
(a) γ versus Particle Velocity in km/sec

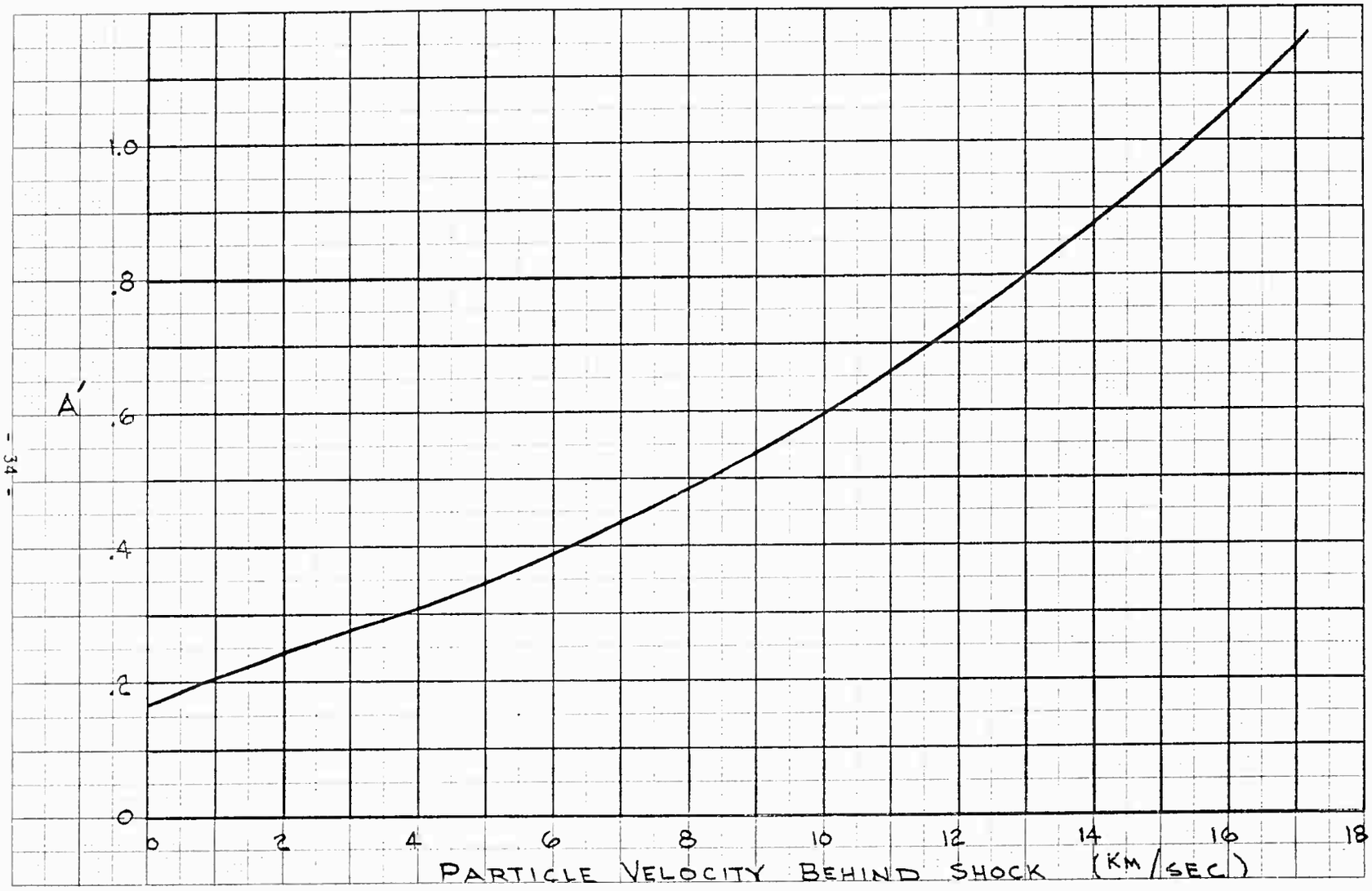

Figure 9. Constants in Isentrope Equation 11 for Aluminum
(b) A' versus Particle Velocity in $^{km}/_{sec}$

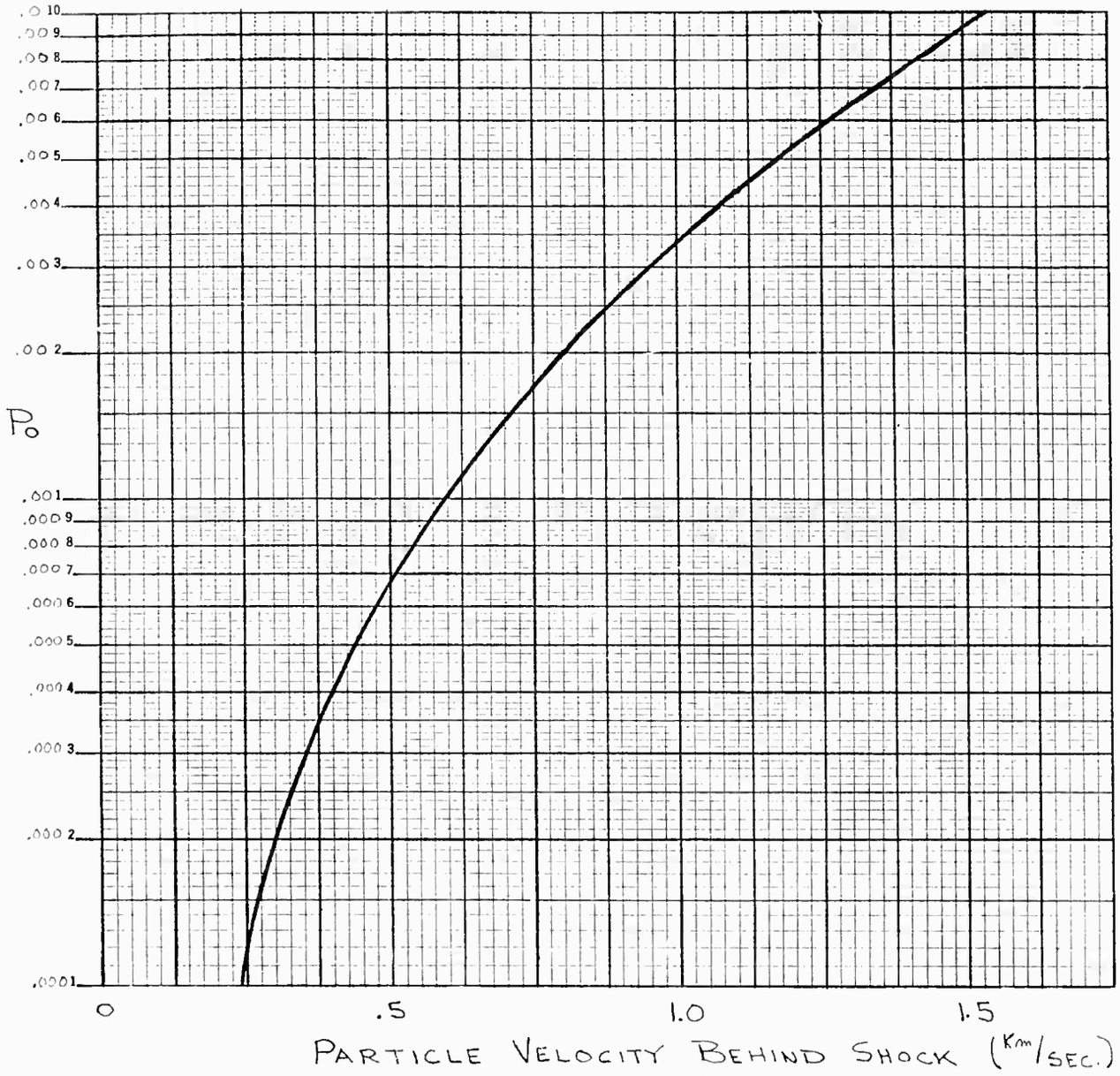

Figure 9. Constants in Isentrope Equation 11 for Aluminum

(c) P_o versus Particle Velocity in $^{km}/_{sec}$

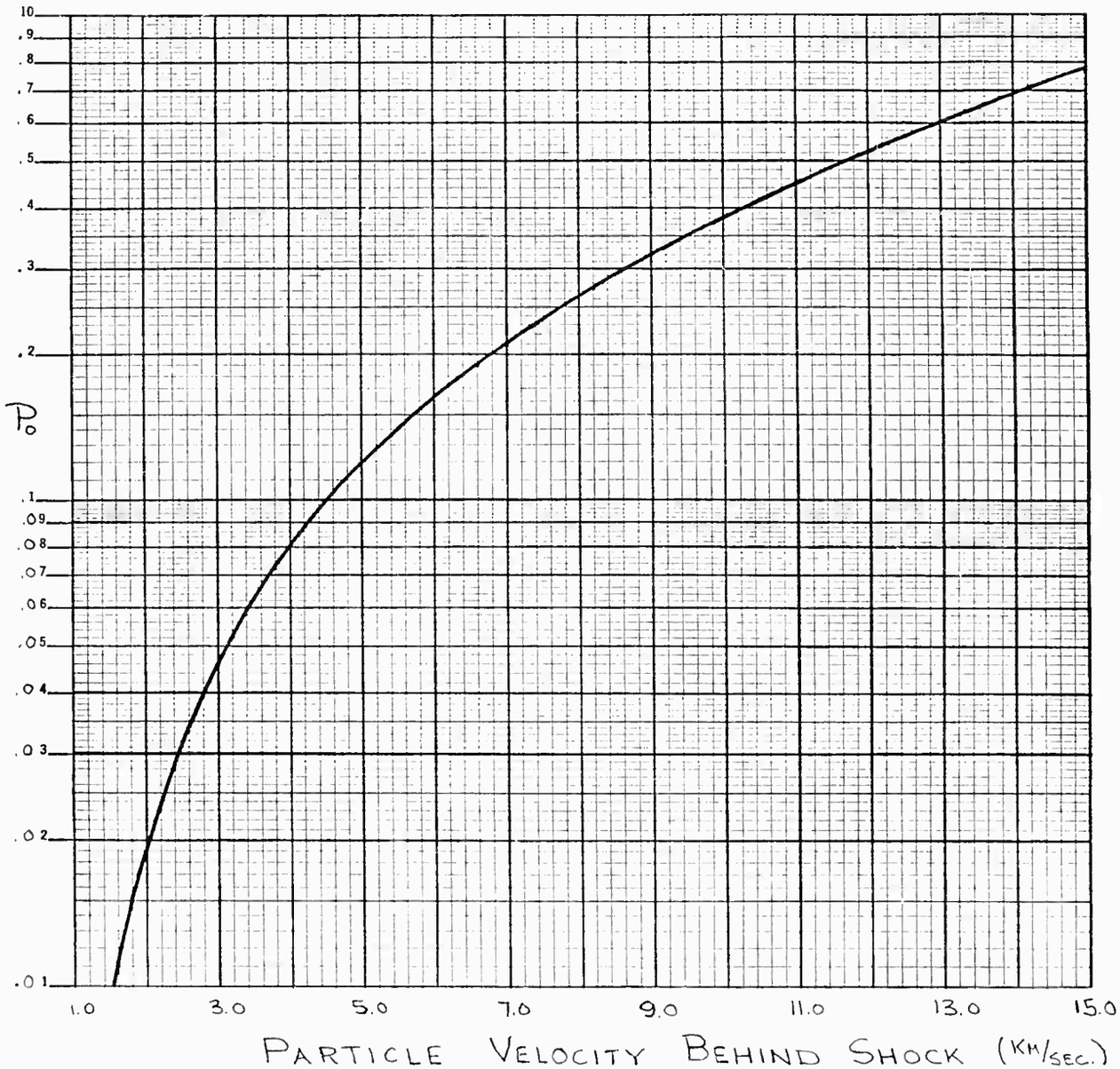

Figure 9. Constants in Isentrope Equation 11 for Aluminum

(c) P_o versus Particle Velocity in $^{km}/_{sec}$ (continued)

TABLE 1 EQUATION OF STATE

Data (for Aluminum)

The data contained in this table has been calculated from the following equation:

$$P = \left[a + \frac{b}{\frac{E}{E_o \eta^2} + 1} \right] \frac{E}{V} + A\mu + B\mu^2 \cdot \qquad (16)$$

where, a= .5 A= .752 Mb. E_o= .05 $\left(\frac{mb - cm^3}{gr.}\right)$
b= 1.63 B= .65 Mb.

u	U	P_H	ρ_o / ρ_H	C_H	γ	A'	P_o	Z
.02	5.306	.003	.996	5.28	4.349	.171	.0000	5.30
.04	5.335	.006	.993	5.32	4.339	.171	.0000	5.36
.06	5.365	.009	.989	5.35	4.329	.172	.0000	5.41
.08	5.395	.012	.985	5.39	4.318	.173	.0000	5.47
.10	5.424	.015	.982	5.43	4.308	.174	.0000	5.53
.12	5.454	.018	.978	5.47	4.298	.174	.0000	5.59
.14	5.483	.021	.974	5.50	4.289	.175	.0000	5.64
.16	5.513	.024	.971	5.54	4.279	.176	.0000	5.70
.18	5.543	.027	.968	5.57	4.269	.176	.0000	5.75
.20	5.572	.030	.964	5.61	4.259	.177	.0000	5.81
.22	5.602	.033	.961	5.65	4.250	.178	.0001	5.87
.24	5.631	.036	.957	5.68	4.241	.178	.0001	5.92
.26	5.661	.040	.954	5.72	4.231	.179	.0002	5.98
.28	5.690	.043	.951	5.75	4.222	.180	.0002	6.03
.30	5.720	.046	.948	5.79	4.213	.181	.0002	6.09
.32	5.750	.050	.944	5.82	4.204	.181	.0003	6.14
.34	5.779	.053	.941	5.86	4.195	.182	.0003	6.20
.36	5.809	.056	.938	5.89	4.186	.183	.0003	6.25
.38	5.838	.060	.935	5.93	4.178	.183	.0004	6.31
.40	5.868	.063	.932	5.96	4.169	.184	.0004	6.36
.42	5.898	.067	.929	6.00	4.161	.185	.0005	6.42
.44	5.927	.070	.926	6.03	4.152	.185	.0005	6.47
.46	5.957	.074	.923	6.06	4.144	.186	.0006	6.52
.48	5.986	.078	.920	6.10	4.135	.187	.0006	6.58
.50	6.016	.081	.917	6.13	4.127	.188	.0007	6.63
.52	6.046	.085	.914	6.16	4.119	.188	.0007	6.68
.54	6.075	.089	.911	6.20	4.111	.189	.0008	6.74
.56	6.105	.092	.908	6.23	4.103	.190	.0009	6.79
.58	6.134	.096	.905	6.26	4.095	.190	.0009	6.84
.60	6.164	.100	.903	6.29	4.087	.191	.0010	6.89
.62	6.193	.104	.900	6.33	4.080	.192	.0011	6.95
.64	6.223	.108	.897	6.36	4.072	.192	.0012	7.00
.66	6.253	.111	.894	6.39	4.064	.193	.0013	7.05
.68	6.282	.115	.892	6.42	4.057	.194	.0014	7.10
.70	6.312	.119	.889	6.45	4.049	.195	.0015	7.15

TABLE 1, cont.

u	U	P_H	ρ_o/ρ_H	C_H	γ	A'	P_o	Z
.72	6.341	.123	.886	6.49	4.042	.195	.0016	7.21
.74	6.371	.127	.884	6.52	4.035	.196	.0017	7.26
.76	6.401	.131	.881	6.55	4.028	.197	.0018	7.31
.78	6.430	.135	.879	6.58	4.020	.197	.0019	7.36
.80	6.460	.140	.876	6.61	4.013	.198	.0020	7.41
.82	6.489	.144	.874	6.64	4.006	.199	.0021	7.46
.84	6.519	.148	.871	6.67	3.999	.199	.0022	7.51
.86	6.549	.152	.869	6.70	3.992	.200	.0024	7.56
.88	6.578	.156	.866	6.73	3.985	.201	.0025	7.61
.90	6.608	.161	.864	6.76	3.979	.202	.0026	7.66
.92	6.637	.165	.861	6.79	3.972	.202	.0028	7.71
.94	6.667	.169	.859	6.82	3.965	.203	.0029	7.76
.96	6.696	.174	.857	6.85	3.959	.204	.0031	7.81
.98	6.726	.178	.854	6.88	3.952	.204	.0032	7.86
1.00	6.756	.182	.852	6.91	3.946	.205	.0034	7.91
1.02	6.785	.187	.850	6.94	3.939	.206	.0036	7.96
1.04	6.815	.191	.847	6.97	3.933	.206	.0037	8.01
1.05	6.848	.194	.847	7.00	3.931	.207	.0039	8.05
1.10	6.918	.205	.841	7.07	3.915	.209	.0043	8.17
1.15	6.988	.217	.835	7.14	3.899	.210	.0048	8.29
1.20	7.058	.229	.830	7.21	3.884	.212	.0053	8.41
1.25	7.127	.241	.825	7.28	3.869	.214	.0059	8.53
1.30	7.197	.253	.819	7.35	3.854	.216	.0065	8.65
1.35	7.267	.265	.814	7.42	3.840	.217	.0072	8.77
1.40	7.337	.277	.809	7.48	3.826	.219	.0078	8.88
1.45	7.407	.290	.804	7.55	3.812	.221	.0086	9.00
1.50	7.477	.303	.799	7.62	3.798	.223	.0093	9.12
1.55	7.547	.316	.795	7.68	3.785	.224	.0102	9.23
1.60	7.616	.329	.790	7.75	3.772	.226	.0110	9.35
1.65	7.686	.342	.785	7.81	3.759	.228	.0119	9.46
1.70	7.756	.356	.781	7.88	3.746	.230	.0129	9.58
1.75	7.826	.370	.776	7.94	3.734	.231	.0139	9.69
1.80	7.896	.384	.772	8.00	3.722	.233	.0150	9.80
1.85	7.966	.398	.768	8.06	3.710	.235	.0161	9.91
1.90	8.036	.412	.764	8.13	3.698	.237	.0173	10.03
1.95	8.105	.427	.759	8.19	3.686	.238	.0185	10.14
2.00	8.175	.441	.755	8.25	3.675	.240	.0198	10.25
2.05	8.245	.456	.751	8.31	3.664	.242	.0212	10.36
2.10	8.315	.471	.747	8.36	3.653	.241	.0208	10.46
2.15	8.385	.487	.744	8.42	3.642	.243	.0219	10.57
2.20	8.455	.502	.740	8.49	3.631	.245	.0230	10.69
2.25	8.525	.518	.736	8.55	3.621	.246	.0242	10.80
2.30	8.594	.534	.732	8.61	3.611	.248	.0254	10.91
2.35	8.664	.550	.729	8.67	3.601	.250	.0266	11.02
2.40	8.734	.566	.725	8.73	3.591	.252	.0279	11.13
2.45	8.804	.582	.722	8.79	3.581	.253	.0292	11.24
2.50	8.874	.599	.718	8.85	3.571	.255	.0305	11.35
2.55	8.944	.616	.715	8.90	3.562	.257	.0319	11.45
2.60	9.014	.633	.712	8.96	3.552	.259	.0333	11.56
2.65	9.084	.650	.708	9.02	3.543	.261	.0348	11.67
2.70	9.153	.667	.705	9.08	3.534	.262	.0363	11.78
2.75	9.223	.685	.702	9.14	3.525	.264	.0378	11.89
2.80	9.293	.703	.699	9.19	3.516	.266	.0394	11.99

TABLE 1, cont.

u	U	P_H	ρ_o/ρ_H	C_H	γ	A'	P_o	Z
2.85	9.377	.722	.696	9.27	3.515	.268	.0416	12.12
2.90	9.441	.739	.693	9.32	3.505	.269	.0430	12.22
2.95	9.505	.757	.690	9.37	3.495	.271	.0444	12.32
3.00	9.569	.775	.686	9.42	3.485	.273	.0458	12.42
3.05	9.632	.793	.683	9.48	3.476	.275	.0473	12.53
3.10	9.696	.812	.680	9.53	3.467	.276	.0488	12.63
3.15	9.760	.830	.677	9.58	3.457	.278	.0502	12.73
3.20	9.824	.849	.674	9.63	3.448	.280	.0518	12.83
3.25	9.888	.868	.671	9.68	3.439	.282	.0533	12.93
3.30	9.951	.887	.668	9.73	3.430	.283	.0549	13.03
3.35	10.015	.906	.666	9.78	3.421	.285	.0565	13.13
3.40	10.079	.925	.663	9.83	3.413	.287	.0581	13.23
3.45	10.143	.945	.660	9.88	3.404	.289	.0598	13.33
3.50	10.207	.965	.657	9.93	3.396	.291	.0614	13.43
3.55	10.270	.984	.654	9.98	3.387	.292	.0631	13.53
3.60	10.334	1.004	.652	10.03	3.379	.294	.0649	13.63
3.65	10.398	1.025	.649	10.08	3.371	.296	.0666	13.73
3.70	10.462	1.045	.646	10.13	3.363	.298	.0684	13.83
3.75	10.526	1.066	.644	10.18	3.355	.299	.0702	13.93
3.80	10.589	1.086	.641	10.23	3.347	.301	.0721	14.03
3.85	10.653	1.107	.639	10.27	3.339	.303	.0739	14.12
3.90	10.717	1.129	.636	10.32	3.331	.305	.0758	14.22
3.95	10.781	1.150	.634	10.37	3.324	.306	.0778	14.32
4.00	10.845	1.171	.631	10.42	3.316	.308	.0797	14.42
4.05	10.908	1.193	.629	10.46	3.309	.310	.0817	14.51
4.10	10.972	1.215	.626	10.51	3.301	.312	.0837	14.61
4.15	11.036	1.237	.624	10.56	3.294	.314	.0857	14.71
4.20	11.100	1.259	.622	10.61	3.287	.315	.0878	14.81
4.25	11.164	1.281	.619	10.65	3.280	.317	.0899	14.90
4.30	11.227	1.304	.617	10.70	3.272	.319	.0920	15.00
4.35	11.291	1.326	.615	10.74	3.265	.321	.0941	15.09
4.40	11.355	1.349	.613	10.79	3.258	.322	.0963	15.19
4.45	11.419	1.372	.610	10.84	3.251	.324	.0985	15.29
4.50	11.483	1.395	.608	10.88	3.245	.326	.1008	15.38
4.55	11.546	1.418	.606	10.93	3.238	.328	.1030	15.48
4.60	11.610	1.442	.604	10.97	3.231	.329	.1053	15.57
4.65	11.674	1.466	.602	11.02	3.224	.331	.1076	15.67
4.70	11.738	1.490	.600	11.06	3.218	.333	.1100	15.76
4.75	11.802	1.514	.598	11.13	3.211	.339	.1096	15.88
4.80	11.865	1.538	.595	11.18	3.205	.341	.1115	15.98
4.85	11.929	1.562	.593	11.23	3.198	.342	.1135	16.08
4.90	11.993	1.587	.591	11.28	3.192	.344	.1154	16.18
4.95	12.057	1.611	.589	11.34	3.186	.346	.1174	16.29
5.00	12.121	1.636	.587	11.39	3.179	.348	.1194	16.39
5.05	12.184	1.661	.586	11.44	3.173	.350	.1214	16.49
5.10	12.248	1.687	.584	11.49	3.167	.352	.1234	16.59
5.15	12.312	1.712	.582	11.54	3.161	.354	.1255	16.69
5.20	12.376	1.738	.580	11.59	3.155	.355	.1275	16.79
5.25	12.440	1.763	.578	11.64	3.149	.357	.1296	16.89
5.30	12.503	1.789	.576	11.69	3.143	.359	.1316	16.99
5.35	12.567	1.815	.574	11.74	3.137	.361	.1337	17.09
5.40	12.631	1.842	.572	11.79	3.131	.363	.1358	17.19
5.45	12.695	1.868	.571	11.84	3.125	.365	.1379	17.29

TABLE 1, cont.

u	U	P_H	ρ_o / ρ_H	C_H	γ	A'	P_o	Z
5.50	12.759	1.895	.569	11.89	3.119	.367	.1401	17.39
5.55	12.822	1.921	.567	11.94	3.114	.369	.1422	17.49
5.60	12.886	1.948	.565	11.99	3.108	.371	.1444	17.59
5.65	12.950	1.976	.564	12.04	3.102	.373	.1465	17.69
5.70	13.014	2.003	.562	12.09	3.097	.375	.1487	17.79
5.80	13.159	2.061	.559	12.09	3.085	.380	.1534	17.89
5.90	13.280	2.115	.556	12.17	3.074	.384	.1577	18.07
6.00	13.401	2.171	.552	12.25	3.064	.388	.1622	18.25
6.10	13.522	2.227	.549	12.34	3.053	.392	.1667	18.44
6.20	13.644	2.284	.546	12.42	3.043	.396	.1712	18.62
6.30	13.765	2.341	.542	12.50	3.033	.400	.1758	18.80
6.40	13.886	2.400	.539	12.58	3.023	.405	.1805	18.98
6.50	14.008	2.458	.536	12.67	3.013	.409	.1852	19.17
6.60	14.129	2.518	.533	12.75	3.003	.414	.1899	19.35
6.70	14.250	2.578	.530	12.83	2.993	.418	.1947	19.53
6.80	14.372	2.639	.527	12.91	2.984	.423	.1996	19.71
6.90	14.493	2.700	.524	12.99	2.974	.427	.2045	19.89
7.00	14.614	2.762	.521	13.07	2.965	.432	.2095	20.07
7.10	14.735	2.825	.518	13.15	2.956	.436	.2145	20.25
7.20	14.857	2.888	.515	13.23	2.947	.441	.2196	20.43
7.30	14.978	2.952	.513	13.30	2.938	.446	.2247	20.60
7.40	15.099	3.017	.510	13.38	2.929	.451	.2298	20.78
7.50	15.221	3.082	.507	13.46	2.920	.456	.2351	20.96
7.60	15.342	3.148	.505	13.54	2.911	.461	.2404	21.14
7.70	15.463	3.215	.502	13.62	2.903	.466	.2457	21.32
7.80	15.585	3.282	.500	13.69	2.894	.471	.2511	21.49
7.90	15.706	3.350	.497	13.77	2.886	.476	.2565	21.67
8.00	15.827	3.419	.495	13.85	2.878	.481	.2620	21.85
8.10	15.948	3.488	.492	13.92	2.869	.486	.2675	22.02
8.20	16.070	3.558	.490	14.00	2.861	.491	.2731	22.20
8.30	16.191	3.628	.487	14.07	2.853	.496	.2788	22.37
8.40	16.312	3.700	.485	14.15	2.845	.502	.2845	22.55
8.50	16.434	3.772	.483	14.22	2.837	.507	.2902	22.72
8.60	16.555	3.844	.481	14.30	2.830	.512	.2960	22.90
8.70	16.676	3.917	.478	14.37	2.822	.518	.3019	23.07
8.80	16.798	3.991	.476	14.45	2.814	.523	.3078	23.25
8.90	16.919	4.066	.474	14.52	2.807	.529	.3137	23.42
9.00	17.040	4.141	.472	14.60	2.799	.534	.3198	23.60
9.10	17.161	4.217	.470	14.67	2.792	.540	.3258	23.77
9.20	17.283	4.293	.468	14.74	2.784	.546	.3319	23.94
9.30	17.404	4.370	.466	14.82	2.777	.552	.3381	24.12
9.40	17.525	4.448	.464	14.89	2.770	.557	.3443	24.29
9.50	17.647	4.526	.462	14.96	2.763	.563	.3506	24.46
9.60	17.768	4.605	.460	15.03	2.756	.569	.3569	24.63
9.70	17.889	4.685	.458	15.11	2.749	.575	.3633	24.81
9.80	18.011	4.766	.456	15.18	2.742	.581	.3697	24.98
9.90	18.132	4.847	.454	15.25	2.735	.587	.3762	25.15
10.00	18.253	4.928	.452	15.32	2.728	.593	.3828	25.32
10.10	18.374	5.011	.450	15.39	2.721	.599	.3894	25.49
10.20	18.496	5.094	.449	15.46	2.714	.605	.3960	25.66
10.30	18.617	5.177	.447	15.53	2.708	.612	.4027	25.83
10.40	18.738	5.262	.445	15.60	2.701	.618	.4094	26.00
10.50	18.860	5.347	.443	15.68	2.694	.624	.4162	26.18

TABLE 1, cont.

u	U	P_H	ρ_o/ρ_H	C_H	γ	A'	P_o	Z
10.60	18.981	5.432	.442	15.75	2.688	.631	.4231	26.35
10.70	19.102	5.519	.440	15.82	2.681	.637	.4300	26.52
10.80	19.224	5.606	.438	15.89	2.675	.644	.4369	26.69
10.90	19.345	5.693	.437	15.95	2.669	.650	.4440	26.85
11.00	19.466	5.781	.435	16.02	2.662	.657	.4510	27.02
11.10	19.587	5.870	.433	16.09	2.656	.663	.4581	27.19
11.20	19.709	5.960	.432	16.16	2.650	.670	.4653	27.36
11.30	19.830	6.050	.430	16.23	2.644	.677	.4725	27.53
11.40	19.951	6.141	.429	16.30	2.638	.684	.4798	27.70
11.50	20.073	6.233	.427	16.37	2.632	.690	.4871	27.87
11.60	20.194	6.325	.426	16.44	2.626	.697	.4945	28.04
11.70	20.315	6.418	.424	16.50	2.620	.704	.5019	28.20
11.80	20.437	6.511	.423	16.57	2.614	.711	.5094	28.37
11.90	20.558	6.605	.421	16.64	2.608	.718	.5169	28.54
12.00	20.679	6.700	.420	16.71	2.602	.725	.5245	28.71
12.10	20.800	6.796	.418	16.77	2.596	.732	.5321	28.87
12.20	20.922	6.892	.417	16.84	2.590	.739	.5398	29.04
12.30	21.043	6.988	.415	16.91	2.585	.747	.5476	29.21
12.40	21.164	7.086	.414	16.97	2.579	.754	.5554	29.37
12.50	21.286	7.184	.413	17.04	2.573	.761	.5632	29.54
12.60	21.407	7.283	.411	17.11	2.568	.769	.5711	29.71
12.70	21.528	7.382	.410	17.17	2.562	.776	.5791	29.87
12.80	21.650	7.482	.409	17.24	2.557	.783	.5871	30.04
12.90	21.771	7.583	.407	17.31	2.551	.791	.5951	30.21
13.00	21.892	7.684	.406	17.37	2.546	.798	.6032	30.37
13.10	22.013	7.786	.405	17.44	2.540	.806	.6114	30.54
13.20	22.135	7.889	.404	17.50	2.535	.814	.6196	30.70
13.30	22.256	7.992	.402	17.57	2.530	.821	.6279	30.87
13.40	22.377	8.096	.401	17.63	2.525	.829	.6362	31.03
13.50	22.499	8.201	.400	17.70	2.519	.837	.6446	31.20
13.60	22.620	8.306	.399	17.76	2.514	.845	.6530	31.36
13.70	22.741	8.412	.398	17.83	2.509	.853	.6615	31.53
13.80	22.863	8.519	.396	17.89	2.504	.861	.6700	31.69
13.90	22.984	8.626	.395	17.96	2.499	.869	.6786	31.86
14.00	23.105	8.734	.394	18.02	2.493	.877	.6872	32.02
14.10	23.226	8.842	.393	18.08	2.488	.885	.6959	32.18
14.20	23.348	8.952	.392	18.15	2.483	.893	.7046	32.35
14.30	23.469	9.061	.391	18.21	2.478	.901	.7134	32.51
14.40	23.590	9.172	.390	18.28	2.473	.909	.7223	32.68
14.50	23.712	9.283	.388	18.34	2.468	.918	.7311	32.84
14.60	23.833	9.395	.387	18.40	2.464	.926	.7401	33.00
14.70	23.954	9.507	.386	18.47	2.459	.934	.7491	33.17
14.80	24.076	9.621	.385	18.53	2.454	.943	.7581	33.33
14.90	24.197	9.734	.384	18.59	2.449	.951	.7673	33.49
15.00	24.318	9.849	.383	18.65	2.444	.960	.7764	33.65
15.10	24.439	9.964	.382	18.72	2.439	.968	.7856	33.82
15.20	24.561	10.080	.381	18.78	2.435	.977	.7949	33.98
15.30	24.682	10.196	.380	18.84	2.430	.986	.8042	34.14
15.40	24.803	10.313	.379	18.90	2.425	.994	.8136	34.30
15.50	24.925	10.431	.378	18.97	2.421	1.003	.8230	34.47
15.60	25.046	10.549	.377	19.03	2.416	1.012	.8324	34.63
15.70	25.167	10.668	.376	19.09	2.412	1.021	.8420	34.79
15.80	25.289	10.788	.375	19.15	2.407	1.030	.8515	34.95

TABLE 1, cont.

u	U	P_H	ρ_c / ρ_H	C_H	γ	A'	P_o	Z
15.90	25.410	10.908	.374	19.21	2.402	1.039	.8612	35.11
16.00	25.531	11.029	.373	19.28	2.398	1.048	.8709	35.28
16.10	25.652	11.151	.372	19.34	2.393	1.057	.8806	35.44
16.20	25.774	11.273	.371	19.40	2.389	1.066	.8904	35.60
16.30	25.895	11.396	.371	19.46	2.384	1.075	.9002	35.76
16.40	26.016	11.520	.370	19.52	2.380	1.084	.9101	35.92
16.50	26.138	11.644	.369	19.58	2.376	1.094	.9200	36.08
16.60	26.259	11.769	.368	19.64	2.371	1.103	.9300	36.24
16.70	26.380	11.895	.367	19.70	2.367	1.112	.9401	36.40
16.80	26.502	12.021	.366	19.76	2.363	1.122	.9502	36.56
16.90	26.623	12.148	.365	19.82	2.358	1.131	.9603	36.72
17.00	26.744	12.276	.364	19.88	2.354	1.141	.9705	36.88
17.10	26.865	12.404	.363	19.94	2.350	1.150	.9808	37.04
17.20	26.987	12.533	.363	20.00	2.346	1.160	.9911	37.20
17.30	27.108	12.662	.362	20.06	2.341	1.169	1.0015	37.36
17.40	27.229	12.792	.361	20.12	2.337	1.179	1.0119	37.52
17.50	27.351	12.923	.360	20.18	2.333	1.189	1.0224	37.68
17.60	27.472	13.055	.359	20.24	2.329	1.199	1.0329	37.84

REGION	km/sec μ	km/sec c	megabars p
1	0	5.27	0
2	14.10	18.08	8.84
3	0	7.50	.30
4	12.50	16.88	6.96
5	11.00	15.76	5.52
6	9.00	14.26	3.92
7	7.00	12.76	2.65
8	5.00	11.27	1.64
9	2.50	9.40	0.85
10	12.38	16.97	7.06
11	10.87	15.84	5.62
12	8.88	14.34	4.00
20	12.38	16.96	7.06
21	10.94	15.81	5.57
22	8.93	14.31	3.97
30	10.94	15.81	5.57
31	8.98	14.25	3.93
32	8.98	14.27	3.93
50	10.85	15.88	5.65
51	8.90	14.31	4.01
70	10.85	15.92	5.65
71	8.96	14.27	3.95
90	8.96	14.36	3.95

TABLE 2 - PARTIAL LIST OF STATE PROPERTIES

(Regions Correspond to Figure 4)

initial data:

impact velocity = 28.2 km/sec.

$u_1 = o$, $p_1 = o$, $c_1 = 5.275$ km/sec

REGIONS COMPARED		Properties within simple wave		Properties behind shock		change in u	change in c	change in $u + c$
Region in simple wave (no subscript)	Region behind shock (subscript H)	u (km/sec)	c (km/sec)	u_H (km/sec)	c_H (km/sec)	$\frac{u_H - u}{u}$	$\frac{c_H - c}{c}$	$\frac{(u+c)_H - (u+c)}{(u+c)}$
4	20	12.5	16.88	12.38	16.97	- .960%	.533%	- .103%
5	70	11.0	15.76	10.86	15.92	-1.270%	1.030%	.070%
6	120	9.0	14.26	8.85	14.48	-1.670%	1.540%	.300%

TABLE 3a

Comparison of u, c, and $u + c$ along a straight line in graphical solution (for aluminum with impact velocity of 28.2 km/sec.)

REGIONS COMPARED		Properties within simple wave		Properties behind shock		change in u $\frac{u_H - u}{u}$	change in c $\frac{c_H - c}{c}$	change in $u+c$ $\frac{(u+c)_H - (u+c)}{(u+c)}$
Region in simple wave (no subscript)	Region behind shock (subscript H)	u (km/sec)	c (km/sec)	u_H (km/sec)	c_H (km/sec)			
4	20	.516	.488	.510	.472	- 1.16%	- 3.28%	- 2.19%
5	70	.430	.470	.423	.445	- 1.63%	- 5.32%	- 3.56%
6	120	.344	.453	.338	.420	- 1.74%	- 7.28%	- 4.89%

TABLE 3b.

Comparison of u, c, and u + c along a straight line in the graphical solution (for an ideal gas with impact velocity of 1.22 km/sec, $c_1 = .344$ km/sec, $\gamma = 1.4$)

IX. REFERENCES

1. Walsh, J. M., and Tillotson, J. H., "Hydrodynamics of Hypervelocity Impact, General Atomic, GA-3827, January 22, 1963.

2. Bjork, Robert L., "Review of Physical Processes in Hypervelocity Impact and Penetration," Proc. of the Sixth Symposium on Hypervelocity Impact, Vol. II, Part I, August, 1963.

3. Rae, W. J., and Kirchner, H.P., "Final Report on a Study of Meteoroid Impact Phenomena," Cornell Aeronautical Laboratory, Inc., Report No. RM-1655-M-4, February, 1963.

4. Herrmann, Walter, Witner, Emmett A., Percy, John H., and Jones, Arlon H., "Stress Wave Propagation and Spallation in Uniaxial Strain," ASD-TDR-62-399, Air Force Systems Command, Wright Patterson Air Force Base, September, 1962.

5. Fowles, G. R., "Attenuation of the Shock Wave Produced in a Solid by a Flying Plate," Journ. Applied Physics, Vol. 31, No. 4, pp. 655-661, April, 1960.

6. Tillotson, J. H., "Metallic Equations of State for Hypervelocity Impact," General Atomic, GA-3216, July 18, 1962.

7. Murnaghan, F. D., "Finite Deformation of an Elastic Solid (John Wiley and Sons, Inc., New York, 1951).

8. Courant, R., and Friedrichs, K. O., "Supersonic Flow and Shock Waves," Interscience Publishers Inc., New York, 1948.

9. Shapiro, Ascher H., "The Dynamics and Thermodynamics of Compressible Fluid Flow," Vol. II., The Ronald Press Company, New York, 1954.

10. Chou, P. C., Karpp, Robert R., and Zajac, Lawrence J., "Decay of Strong Plane Shocks in an Ideal Gas," Drexel Institute of Technology Report No 160-3, January, 1964

11. Al'tshuler, L. V., Kormer, S. B., Brazhnik, M. I., Vladimirov, L. A., Speranskaya, M.P., and Funtikov, A.I., "The Isentropic Compressibility of Aluminum, Copper, Lead, and Iron at High Pressures," Soviet Physics JETP, Vol II, No. 4, October, 1960

APPENDIX A--Discussion of Table I

Equation of State Data

In this appendix, the equation of state computational procedure is outlined. The basic equations involved are given in Sections III and IV.

Table I contains the equation of state data for aluminum calculated from equation 16,

$$P = \left[a + \frac{b}{\frac{E}{E_o \eta^2} + 1}\right] \frac{E}{V} + A\mu + B\mu^2 \qquad (16)$$

Values for the constants a, b, E_o, A and B, as determined in reference 6, are listed in Table I. Combining equations (1), (2), (3), and (16) with $u_x = o$, and dropping the subscript "y", we can obtain the shock Hugoniot relation $P = P_H(\rho)$. Data of this Hugoniot pressure-density relation are listed in Table I under P_H and ρ_H. The corresponding values for U and u are also given.

The isentrope is obtained by numerically integrating equation (16) with $E = \int - PdV$. This data is not shown in Table I. (The data for a few isentropes is tabulated in reference 6 for several metals). The values of A', γ, P_o are obtained by fitting equation (11) to each isentrope. These values for each isentrope are shown in Table I on the same line with the particular P_H and ρ_H corresponding to the intersection point of the isentrope curve and the Hugoniot curve.

The sound velocity can be obtained either by numerically differentiating the data from equations (16) and (9), or it can be obtained from equation (12). The results from the latter equation (12) are shown in Table I.

In figures 9a to 9c, the constants A', γ, and P_o for the isentropes are also plotted as functions of the particle velocity immediately behind the shock, (i.e., at the intersection of the isentropes and the Hugoniot).